Neural Computing and Applications (2023) 35:15429–15446
https://doi.org/10.1007/s00521-023-08361-y

ORIGINAL ARTICLE

Quantized neural adaptive finite-time preassigned performance control for interconnected nonlinear systems

Xiaona Song[1] · Peng Sun[1] · Shuai Song[1] · Vladimir Stojanovic[2]

Received: 26 July 2022 / Accepted: 13 February 2023 / Published online: 12 April 2023

Abstract
In this article, the issue of neural adaptive decentralized finite-time prescribed performance (FTPP) control is investigated for interconnected nonlinear time-delay systems. First, to bypass the potential singularity difficulties, the hyperbolic tangent function and the radial basis function neural networks are integrated to handle the unknown nonlinear items. Then, an adaptive FTPP control strategy is developed, where an improved fractional-order filter is applied to tackle the tremendous "amount of calculation" and eliminate the filter error simultaneously. Furthermore, by considering the impact of bandwidth limitation, an adaptive self-triggered control law is designed, in which the next trigger instant is determined through the current information. Ultimately, it can be demonstrated that the proposed control scheme not only guarantees that all states of the closed-loop system are semi-globally uniformly ultimately bounded, but also that the system output is confined to a small area in finite time. Two simulation examples are carried out to verify the effectiveness and superiority of the proposed method.

Keywords Decentralized control · Finite-time prescribed performance · Input quantization · Interconnected nonlinear time-delay systems · Self-triggered · Unmodeled dynamics

1 Introduction

Given that some practical systems, such as robotic systems and industrial process systems, etc, are modeled as interconnected nonlinear systems. Therefore, the investigation of interconnected nonlinear systems has attracted widespread interest from scholars. Initially, the centralized control approach is impractical and suffers from the computational burden of redundancy due to the utilization of overall state information. Notably, the decentralized-based adaptive backstepping control schemes [1–3] in each subsystem have capable of independently handling the control assignment of the interconnected system via its local information. Meanwhile, the majority of existing decentralized control results require that the interconnection term of the interconnected system contains all states of the entire interconnected system, which is referred to as strong interconnections. Hence, an adaptive decentralized control method was investigated for interconnected nonlinear systems with strong interconnections in [4]. Due to the existence of unknown nonlinearities in interconnected nonlinear systems, with the aid of radial basis function neural networks (RBFNNs) and fuzzy logic systems, the adaptive decentralized control schemes were presented in [2, 3]. Generally, the backstepping technique entails the issue of complexity in analytical computation stemming from the iterative calculation of the virtual control function. To this end, the dynamic surface control (DSC) schemes [5–7] were proposed to address the explosive calculation by introducing a first-order filter. Although the above DSC methods solve the above issues, filter errors between the filter output and the virtual control function were not eliminated. Thus, the command filter backstepping control (CFBC) methods [8, 9] were constructed by means of an error compensation signal. Meanwhile, Song

✉ Xiaona Song
xiaona97@haust.edu.cn

[1] School of Information Engineering, Henan University of Science and Technology, Kaiyuan Avenu, Luoyang 471023, Henan, China

[2] Department of Automatic Control, Robotics and Fluid Technique, Faculty of Mechanical and Civil Engineering, University of Kragujevac, Kraljevo 36000, Serbia

et al. [10] developed an adaptive fuzzy secure control solution for nonlinear systems, where a fractional-order filter (FOF) was introduced to eradicate the effect of filter errors. Noteworthy, the above CFBC-based control results neglect the impact of the communication burden.

Until today, event-triggered control (ETC) plays an important role in the realm of transmission resource constraints, where the measurement error satisfies the trigger criterion, the control signal will be updated and applied to the system. Targeting the aircraft wing rock motion [11], an adaptive event-triggered control was presented to economize communication resources. [12] discussed the prescribed-time synchronization issue for nonlinear systems via ETC strategy. Unfortunately, the event-triggered mechanism is imposed to continuously monitor the trigger criteria, which requires relatively unavailable hardware situations for industrial applications. With this in mind, an adaptive self-triggered control solution was investigated in [13], which can calculate the next trigger instant following the current information. Meanwhile, [14] reported a neural adaptive self-triggered control method for nonlinear systems with unmeasurable states.

To further handle the limitation of bandwidth in networked control, quantized control was used to degrade the communication rate to satisfy that the system can operate normally within the specified bandwidth. Initially, a logarithmic quantizer was investigated in [15], where the bandwidth of the constrained transmission was alleviated. However, the chattering phenomenon will inevitably occur in the quantization control of continuous-time systems. Soon afterward, the hysteresis quantizer was developed in [16], which can decrease the risk of chattering. In [17], an adaptive fuzzy quantized control was proposed for nonlinear systems. In addition, networked control may result in discontinuous control signals at two trigger instants, which will drastically affect the control system's performance. Hence, it is imperative to concentrate on the trade-off between communication cost and tracking precision.

It is widely acknowledged that prescribed performance control (PPC) enables tracking errors to converge to a predefined range. Particularly, Sun et al. [18] and Song et al. [19] investigated the adaptive CFBC methods for the different nonlinear systems, where transient and steady performances were maintained. In [20], an adaptive PPC scheme was analyzed for nonlinear systems. Soon afterward, an improved performance function in comparison to PPC is proposed, called the finite-time prescribed performance (FTPP) function, which guarantees that the tracking error is confined to a small origin in finite time. In particular, [21] developed a fuzzy adaptive FTPP control strategy for nonlinear systems with dynamic uncertainty. Nevertheless, the above results do not both consider the time delay and unmodeled dynamics that are ubiquitous in modern industrial applications.

Naturally speaking, if this obstacle is not overcome, the system performance will deteriorate and even resulting in the instability of the closed-loop system. Thus, many remarkable results have been reported to ensure the stability of the systems (see [22–26] and reference therein). Among them, by introducing a dynamic signal, an adaptive decentralized tracking control strategy was addressed for nonlinear systems with dynamical uncertainties in [23]. In [24], with the help of Lyapunov–Krasovskii functional, an adaptive neural control scheme was discussed for interconnected nonlinear systems with time delay. Meanwhile, Li et al. [26] developed an adaptive CFBC method for nonlinear time-delay systems.

Guided by the foregoing analysis, this paper developed the neural adaptive FTPP quantized control strategy by utilizing the FOF for interconnected nonlinear time-delay systems with unmodeled dynamics and self-triggered input. The highlights of this article are enumerated below:

1. Different from the event-triggered mechanism [10, 11, 26], the investigated self-triggered control solution was developed, where the next trigger instant was determined by the current information. In addition, the effect of bandwidth limitation was synthesized in the interconnected nonlinear time-delay system as a challenging issue in comparison to [7, 16, 17]. However, the networked control mentioned above may affect the performance of the system. Tactfully, the FTPP function was considered to optimize the transient and steady-state performance of the interconnected nonlinear system.
2. In contrast to the integer-order filter in [9, 18, 26, 27], an improved FOF was introduced such that the tremendous " amount of calculation " was avoided and the filter performance was skillfully enhanced. Unlike [7, 21, 28], which only considered the PPC issue or error compensation signal, the proposed self-triggered quantized control scheme in this paper takes FTPP and error compensation signal into account to eliminate the filter errors simultaneously.
3. To address the potential singularity problem that may exist in interconnected nonlinear systems, hyperbolic tangent functions, and RBFNNs were introduced in [16, 26]. Furthermore, this article extends both time delay and unmodeled dynamics to interconnected nonlinear systems, which makes it applicable to more general situations [3, 7, 23].

2 System formulation

Consider the following interconnected nonlinear time-delay plant

$$\begin{cases} \dot{\psi}_m = & q_m(\psi_m, \check{x}_m), \\ \dot{x}_{m,i} = & x_{m,i+1} + f_{m,i}(\bar{x}_{m,i}) + g_{m,i}(\bar{y}) + \Delta_{m,i}(\check{x}_m, \psi_i) \\ & + h_{m,i}(\bar{x}_{m,i}(t-\tau_{m,i}(t))), \\ \dot{x}_{m,n_m} = & q(u_m) + f_{m,n_m}(\bar{x}_{m,n_m}) + g_{m,n_m}(\bar{y}) + \Delta_{m,n_m}(\check{x}_m, \psi_i) \\ & + h_{m,n_m}(\bar{x}_{m,n_m}(t-\tau_{m,n_m}(t))), \\ y_m = & x_{m,1}, \end{cases} \tag{1}$$

where $\bar{x}_{m,i} = [x_{m,1}, \ldots, x_{m,i}]^T \in R^i$ and $y_m \in R$ are the state vector and output vector of the mth subsystem, respectively. $\check{x}_m = [x_{m,1}, \ldots, x_{m,n_m}]^T \in R^{n_m}$, $\bar{y} = [y_1, \ldots, y_M]^T \in R^M$. $f_{m,i}(\cdot)$ and $h_{m,i}(\cdot)$ with $1 \le m \le M$ and $1 \le i \le n_m$ are the unknown smooth nonlinear functions, $g_{m,i}(\bar{y})$ denotes the unknown smooth interconnected term between the mth subsystem and other subsystems. $\tau_{m,i}(t)$ represents the time-varying delay satisfying $|\tau_{m,i}(t)| \le \bar{\tau}_{m,i} < \infty$ and $|\dot{\tau}_{m,i}(t)| \le \check{\tau}_{m,i} < 1$, where $\bar{\tau}_{m,i} > 0$ and $\check{\tau}_{m,i} > 0$ are constants. The ψ_m-dynamics and $\Delta_{m,i}(\cdot)$ denote the unmodeled dynamics and dynamic disturbances, respectively. q_m and $\Delta_{m,i}(\cdot)$ indicate the Lipschitz continuous functions. $q(u_m)$ and u_m indicate the quantized control signal and quantized input signal. Meanwhile, the hysteresis quantizer is described as follow:

$$q(u_m) = \begin{cases} u_m^w \mathrm{sgn}(u_m), & \frac{u_m^w}{1+\hbar_m} < |u_m| \le u_m^w, \dot{u}_m < 0, \ or \\ & u_m^w < |u_m| \le \frac{u_m^w}{1-\hbar_m}, \dot{u}_m > 0 \\ u_m^w \vartheta_m, & u_m^w < |u_m| \le \frac{u_m^w}{1-\hbar_m}, \dot{u}_m < 0, \ or \\ & \frac{u_m^w}{1-\hbar_m} < |u_m| \le \frac{u_m^w(1+\hbar_m)}{1-\hbar_m}, \dot{u}_m > 0 \\ 0, & 0 \le |u_m| < \frac{u_m^{\min}}{1+\hbar_m}, \dot{u}_m < 0, \ or \\ & \frac{u_m^{\min}}{1+\hbar_m} \le |u_m| \le u_m^{\min}, \dot{u}_m > 0 \\ q(u_m(t^-)), & other\ case, \end{cases}$$

where $\vartheta_m = (1+\hbar_m)\mathrm{sgn}(u_m)$, $u_m^w = \delta_m^{1-w} u_m^{\min}$ $(w = 1, 2, \ldots)$ with $0 < \delta_m < 1$ stands for a measure of quantization density and $\hbar_m = \frac{1-\delta_m}{1+\delta_m}$, $u_m^{\min}$ indicates the scope of the dead-zone for $q(u_m)$ and $q(u_m)$ is in the set $\bigcup_m = (0, \pm u_m^w, \pm u_m^w(1+\hbar_m))$.

To support the controller design, we need the following assumptions, lemmas, and definitions.

Definition 1 [29] Assume $F(t) : [t_0, +\infty) \to R$ is a continuous function together with its fractional derivative of order P_m under Caputo's definition is expressed as:

$$D^{P_m} F(t) = \frac{1}{\Gamma(n_m - P_m)} \int_0^t \frac{F^{n_m}(\tau)}{(t-\tau)^{P_m+1-n_m}} \mathrm{d}\tau,$$

where n_m denotes an integer such that $n_m - 1 \le P_m \le n_m$. $\Gamma(x) = \int_0^{+\infty} \tau^{x-1} e^{-\tau} \mathrm{d}\tau (x > 0)$ denotes Euler's Gamma function with $\Gamma(1) = 1$.

Definition 2 [28] A smooth finite-time performance function (FTPF) $\ell_m(t)$ satisfies the following characteristics: (1) $\ell_m(t) > 0$, (2) $\dot{\ell}_m(t) \le 0$, (3) $\lim_{t \to T_f} \ell_m(t) = \ell_{mT_f} > 0$ and $\ell_m(t) = \ell_{mT_f} > 0$ for any $t > T_f$ with T_f and ℓ_{mT_f} are the settling time and the arbitrarily small constant, respectively.

Lemma 1 [30] *To further analyze the quantization impact, the hysteretic quantizer is reconstructed as* $q(u_m(t)) = (1-\bar{\kappa}_m)u_m(t) + \bar{\kappa}_m \bar{\varsigma}_m(t)$ *such that the nonlinearity function* $\bar{\varsigma}_m(t)$ *satisfies the following inequalities*:

$$(\bar{\varsigma}_m(t))^2 \le \left(\frac{\bar{\kappa}_m + \hbar_m}{\bar{\kappa}_m} u_m(t)\right)^2, \quad \forall |u_m(t)| \ge u_m^{\min},$$

$$(\bar{\varsigma}_m(t))^2 \le \left(\frac{1-\bar{\kappa}_m}{\bar{\kappa}_m} u_m^{\min}\right)^2, \quad \forall |u_m(t)| \le u_m^{\min},$$

where $0 < \bar{\kappa}_m < 1$ *is an adjustable constant to be designed.*

Assumption 1 [31] There exist unknown non-negative smooth functions $\varphi_{m,i1}(\|\bar{x}_{m,i}\|)$ and $\varphi_{m,i2}(\|\psi_i\|)$, the dynamic disturbance $\Delta_{m,i}(\psi_i, \check{x}_m)$ satisfying

$$\Delta_{m,i}(\psi_i, \check{x}_m) \le \varphi_{m,i1}(\|\bar{x}_{m,i}\|) + \varphi_{m,i2}(\|\psi_i\|).$$

Assumption 2 [32] Let us consider the unmodeled dynamics $\dot{\psi}_m = q_m(\psi_m, \check{x}_m)$, which is exponentially input-to-state practically stable (exp-ISpS). Meanwhile, $V_m(\psi_m)$ is an exp-ISpS Lyapunov function (LF) satisfying

$$\begin{aligned} &\Upsilon_{m,1}(|\psi_m|) \le V_m(\psi_m) \le \Upsilon_{m,2}(|\psi_m|), \\ &\frac{\partial V_m(\psi_m)}{\partial \psi_m} q_m(\psi_m, \check{x}_m) \le -r_{m,1} V_m(\psi_m) + \pi_{m0}(\|x_{m,1}\|) + r_{m,2}, \end{aligned} \tag{2}$$

where $\Upsilon_{m,1}, \Upsilon_{m,2}$, and π_{m0} are class K_∞-functions and $r_{m,1} > 0$ and $r_{m,2} > 0$ denote known constants.

Assumption 3 [4] The interconnected term $g_{m,i}(\bar{y})$ has the form of $|g_{m,i}(\bar{y})| \le \sum_{l=1}^M j_{m,l} \aleph_i(\bar{x}_{l,i})$, with $\aleph_i(\bar{x}_{l,i})$ $(i = 1, \ldots, n_m)$ and $j_{m,l}$ denote the unknown continuous function and unknown constant, respectively.

Lemma 2 [31] *Assume exp-ISpS LF* $V_m(\psi_m)$ *satisfies the equation condition* (2)*, then, for* $\forall \bar{r}_{m,1} \in (0, r_{m,1})$*, the initial condition* $\psi_{m0} = \psi_m(t_0)$, $c_0 > 0$, *and the function*

$\bar{\pi}_{m0}(\|y_m\|) \geq \pi_{m0}(\|y_m\|)$, *there exist a finite time* $T_{m0} = T_{m0}(\bar{r}_{m,1}, c_0, \psi_{m0})$, *a non-negative function* $Q(t_0, t)(t \geq t_0)$, *and a dynamic signal expressed as*:

$$\dot{\lambda}_m = -\bar{r}_{m,1}\lambda_m + \bar{\pi}_{m0}(\|x_{m,1}(t)\|) + r_{m,2},\ \lambda_m(t_0) = \lambda_{m0},$$

satisfying $Q(t_0, t) = 0$ for $\forall t \geq t_0 + T_{m0}$

$$V_m(\psi_m(t)) \leq \lambda_m(t) + Q(t_0, t),\ \forall t \geq t_0,$$

where t_0 *denotes the initial time and assume that* $\bar{\pi}_{m0}(\|x_{m,1}(t)\|) = \pi_{m0}(\|x_{m,1}\|)$.

Lemma 3 [33] *For variable* $\varrho \in R$ *and* $\forall \jmath > 0$, *one has*

$$-\varrho\tanh\left(\frac{\varrho}{\jmath}\right) \leq 0, \quad 0 \leq |\varrho| - \varrho\tanh\left(\frac{\varrho}{\jmath}\right) \leq 0.2785\jmath.$$

Lemma 4 [34] *The compact set* Ω_{m_k} *is defined in* $\Omega_{m_k} = \{s_{m,k} \mid\mid s_{m,k} \mid < 0.2554 m_k\}$. Next, for the case of $\forall s_{m,k} \notin \Omega_{m,k}$, the term $1 - 16\tanh^2(s_{m,k}/m_k) \leq 0$ *holds*.

Lemma 5 [35] *Consider the unknown smooth nonlinearities* $f_{m,i}(\bar{z}_{m,i})$ *on the compact set* Ω_X, *which can be approximated by RBFNNs*

$$f_{m,i}(\bar{z}_{m,i}) = W_{m,i}^{\mathrm{T}} S_{m,i}(\bar{z}_{m,i}) + \varepsilon_{m,i},$$

where $W_{m,i}$ *and* $S_{m,i}(\bar{z}_{m,i}) = [\psi_{m,i1}(\bar{z}_{m,i}), \ldots, \psi_{m,iK}(\bar{z}_{m,i})]^{\mathrm{T}}$ *are, respectively, the weight vector and basic function vector, with* $\bar{z}_{m,i}$ *is the input of the RBFNNs,* $K \geq 1$ *is the number of neuron,* $\varepsilon_{m,i}$ *is the approximation error. There exists a positive constant* $\varepsilon_{m,i}^* > 0$ *such that* $\|\varepsilon_{m,i}\| \leq \varepsilon_{m,i}^*$. *Meanwhile, the Gaussian function is expressed as*:

$$\psi_{m,i}^{l}(\bar{z}_{m,i}) = \exp\left[\frac{-(\bar{z}_{m,i} - h_{m,i})^{\mathrm{T}}(\bar{z}_{m,i} - h_{m,i})}{b_{m,i}^2}\right],$$

where $h_{m,i} = \left[h_{m,i1}, \ldots, h_{m,iM}\right]^{\mathrm{T}}$ *and* $b_{m,i}$ *denote the center and width of the basis function, respectively*.

This paper aims at synthesizing a decentralized-based adaptive neural quantized control algorithm for the interconnected nonlinear time-delay system in (1) such that all signals of the resulting closed-loop system (CLS) are semi-globally uniformly ultimately bounded (SGUUB), the system output is confined to a small adjustable region in a finite time interval, and as well as the Zeno phenomenon is ruled out.

3 Main results

In this section, a decentralized-based adaptive self-triggered neural control scheme will be put forward for interconnected nonlinear time-delay systems.

3.1 State transformation

To confine the system output $x_{m,1}$ to the range $(-\ell_m, \ell_m)$, the FTPF can be chosen from Definition 2.

$$\ell_m(t) = \begin{cases} \left(\ell_{m0} - \dfrac{t}{T_f}\right)e^{\left(1-\frac{T_f}{T_f - t}\right)} + \ell_{mT_f}, & t \in [0, T_f), \\ \ell_{mT_f}, & t \in [T_f, +\infty), \end{cases} \tag{3}$$

where $\ell_{m0} > 0$ and $\ell_{mT_f} > 0$ are design parameters.

Furthermore, it can be obtained that $\ell_m(0) = \ell_{m0} + \ell_{mT_f}$ from Definition 2 and (3). The error transformation function with the transformed error $\eth_m$ is selected as:

$$T(\eth_m) = \frac{e^{\eth_m} - e^{-\eth_m}}{e^{\eth_m} + e^{-\eth_m}}, \tag{4}$$

The transformation is defined as:

$$x_{m,1} = \ell_m(t)T(\eth_m), \tag{5}$$

$$\eth_m = T^{-1}\left(\frac{x_{m,1}}{\ell_m}\right) = \frac{1}{2}\ln\left(\frac{x_{m,1}/\ell_m + 1}{1 - x_{m,1}/\ell_m}\right), \tag{6}$$

and

$$\dot{\eth}_m = p_{m,1}\left(\dot{x}_{m,1} - \frac{\dot{\ell}_m x_{m,1}}{\ell_m}\right), \tag{7}$$

where $p_{m,1} = \frac{1}{2\ell_m}\left(\frac{1}{x_{m,1}/\ell_m + 1} - \frac{1}{x_{m,1}/\ell_m - 1}\right)$.

3.2 Controller design

In contrast to the advancement of integer-order calculus [9, 18, 26, 27], fractional-order calculus [36–39] possesses the property of the favorable filter and enhances the freedom of control design attributed to its distinctive historical memory characteristics. In a nutshell, we propose a FOF-based adaptive self-triggered control algorithm for interconnected nonlinear time-delay systems in (1), which can not only overcome the complicated " amount of calculation " but also effectively upgrade the filter performance of the existing results in [9, 18, 26, 27].

Now, the fractional-order filter (FOF) are constructed:

$$\begin{cases} D^{P_m}\beta_{m,1} = I_{m,1}, \\ \quad I_{m,1} = -k_{m,l1}\lceil\beta_{m,1} - \alpha_{m,i-1}\rfloor^{\frac{1}{2}} \\ \qquad\quad - k_{m,l2}\lceil\beta_{m,1} - \alpha_{m,i-1}\rfloor^{\frac{3}{2}} + \beta_{m,2}, \\ D^{P_m}\beta_{m,2} = -k_{m,l3}\lceil\beta_{m,1} - \alpha_{m,i-1}\rfloor^{\frac{1}{2}}, \end{cases} \tag{8}$$

where D^{P_m} indicates the fractional operator with $0 < P_m < 1$ and $k_{m,li}$ $(i = 1, 2, 3)$ is the design parameter. The virtual

control function $\alpha_{m,i-1}$ indicates the filter input, $\zeta_{m,i} = \beta_{m,1}$ and $D^{P_m}\zeta_{m,i} = I_{m,1}$ are the filter output.

Define the change of coordinate as follows:

$$\begin{cases} z_{m,1} = \partial_m, \\ z_{m,i} = x_{m,i} - \zeta_{m,i}, \quad 1 \le m \le N, \\ \xi_{m,i} = \zeta_{m,i} - \alpha_{m,i-1}, \quad i = 2, \ldots, n_m, \end{cases} \tag{9}$$

where $z_{m,i}$ denotes the error surface and $\xi_{m,i}$ denotes the filter error. Additionally, the compensated error signal $s_{m,i}$ with $i = 1, \ldots, n_m$ is designed as follows:

$$s_{m,i} = z_{m,i} - v_{m,i}, \tag{10}$$

where $v_{m,i}$ is the error compensation signal, which can be specifically designed as:

$$\begin{cases} \dot{v}_{m,1} = -c_{m,1}v_{m,1} + p_{m,1}v_{m,2} + p_{m,1}\xi_{m,2}, \\ \dot{v}_{m,i} = -c_{m,i}v_{m,i} - p_{m,i-1}v_{m,i-1} + v_{m,i+1} + \xi_{m,i+1}, \\ \dot{v}_{m,n_m} = -c_{m,n_m}v_{m,n_m} - p_{m,n_m-1}v_{m,n_m-1}, \end{cases} \tag{11}$$

where $v_{m,i}(0) = 0$, $p_{m,i} = 1$ and $c_{m,i} > 0$ $(i = 2, \ldots, n_m)$ denotes the positive design parameters.

The virtual control functions and the adaptive laws are designed for each subsystem $(i = 2, \ldots, n_m - 1)$ as follows:

$$\begin{aligned} \alpha_{m,1} = & -\frac{c_{m,1}}{p_{m,1}} z_{m,1} - \frac{p_{m,1}s_{m,1}}{2a_{m,1}^2}\hat{\Theta}_{m,1}S_{m,1}^{\mathrm{T}}(\cdot)S_{m,1}(\cdot) \\ & + \frac{\dot{\ell}_m x_{m,1}}{\ell_m}, \end{aligned} \tag{12}$$

$$\begin{aligned} \alpha_{m,i} = & -c_{m,i}z_{m,i} - \frac{s_{m,i}}{2a_{m,i}^2}\hat{\Theta}_{m,i}S_{m,i}^{\mathrm{T}}(\cdot)S_{m,i}(\cdot) \\ & - p_{m,i-1}z_{m,i-1}, \end{aligned} \tag{13}$$

$$\begin{aligned} \alpha_{m,n_m} = & \frac{1}{(1-\bar{\kappa}_m)\underline{\zeta}_{m0}}\Big[-c_{m,n_m}z_{m,n_m} \\ & - (1-\bar{\kappa}_m)\mathrm{sgn}(s_{m,n_m})u_m^{\min} \\ & - \frac{s_{m,n_m}}{2a_{m,n_m}^2}\hat{\Theta}_{m,n_m}S_{m,n_m}^{\mathrm{T}}(\cdot)S_{m,n_m}(\cdot) \\ & - p_{m,n_m-1}z_{m,n_m-1}\Big], \end{aligned} \tag{14}$$

$$\dot{\hat{\Theta}}_{m,1} = \mu_{m,1}\left(\frac{p_{m,1}^2 s_{m,1}^2}{2a_{m,1}^2}S_{m,1}^{\mathrm{T}}(\cdot)S_{m,1}(\cdot) - \rho_{m,1}\hat{\Theta}_{m,1}\right), \tag{15}$$

$$\dot{\hat{\Theta}}_{m,i} = \mu_{m,i}\left(\frac{s_{m,i}^2}{2a_{m,i}^2}S_{m,i}^{\mathrm{T}}(\cdot)S_{m,i}(\cdot) - \rho_{m,i}\hat{\Theta}_{m,i}\right), \tag{16}$$

where $c_{m,i}$ and $\rho_{m,i}$ are positive design parameters. Let us define that $\hat{\Theta}_{m,i}$ denotes the estimates of $\Theta_{m,i}$. $\tilde{\Theta}_{m,i} = \Theta_{m,i} - \hat{\Theta}_{m,i}$ being the parameter estimation error with $\Theta_{m,i} = \max_{1 \le i \le n_m}\left\{\left\|W_{m,i}^*\right\|^2\right\}$. Analogous to (16), $\dot{\hat{\Theta}}_{m,n_m}$ can be expressed by replacing i with n_m.

For simplicity, the corresponding abbreviations are considered: $f_{m,i}$ indicates $f_{m,i}(\bar{x}_{m,i})$, $\Delta_{m,i}$ indicates $\Delta_{m,i}(\check{x}_m, \psi_i)$, $g_{m,i}$ indicates $g_{m,i}(\bar{y})$, $h_{m,i}(x_{m,i\tau})$ indicates $h_{m,i}(\bar{x}_{m,i}(t - \tau_{m,i}(t)))$, and $S_{m,i}^{\mathrm{T}}(\cdot)S_{m,i}(\cdot)$ indicates $S_{m,i}^{\mathrm{T}}(\bar{z}_{m,i})S_{m,i}(\bar{z}_{m,i})$.

Proof The specific control design procedures of this paper are expressed in detail as follows.

Step m, 1: From (7) and (9), the time derivative of $z_{m,1}$ yields

$$\dot{z}_{m,1} = p_{m,1}\left(z_{m,2} + \xi_{m,2} + \alpha_{m,1} + f_{m,1} + \Delta_{m,1} + g_{m,1} + h_{m,1}(x_{m,1\tau}) - \frac{\dot{\ell}_m x_{m,1}}{\ell_m}\right). \tag{17}$$

It follows from (10)–(11) that

$$\begin{aligned} \dot{s}_{m,1} = & p_{m,1}\Big(s_{m,2} + v_{m,2} + \xi_{m,2} + \alpha_{m,1} + f_{m,1} + \Delta_{m,1} \\ & + g_{m,1} + h_{m,1}(x_{m,1\tau}) - \frac{\dot{\ell}_m x_{m,1}}{\ell_m}\Big) - \dot{v}_{m,1}. \end{aligned} \tag{18}$$

Now, we consider the following Lyapunov function:

$$V_1 = \sum_{m=1}^{M}\left[\frac{1}{2}s_{m,1}^2 + \frac{1}{2\mu_{m,1}}\tilde{\Theta}_{m,1}^2 + \frac{\lambda_m}{\varrho_{m0}} + \bar{V}_{m,1}\right],$$

where $\mu_{m,1}$ and ϱ_{m0} are positive constants. The Lyapunov–Krasovskii functional is formulated as $\bar{V}_{m,1} = [e^{\kappa_{m,1}\bar{\tau}_{m,1}}/2(1-\check{\tau}_{m,1})]\int_{t-\tau_{m,1}(t)}^{t} e^{-\kappa_{m,1}(t-s)}h_{m,1}^2(x_{m,1}(s))ds$ to tackle the time delay challenge, where $\kappa_{m,1} > 0$ denotes a constant.

Through calculation, one has

$$\begin{aligned} & \dot{\bar{V}}_{m,1} \le -\kappa_{m,1}\bar{V}_{m,1} + \Psi_{m,1} - \frac{1}{2}h_{m,1}^2(x_{m,1\tau}), \\ & p_{m,1}s_{m,1}h_{m,1}(x_{m,1\tau}) \le \frac{1}{2}p_{m,1}^2 s_{m,1}^2 + \frac{1}{2}h_{m,1}^2(x_{m,1\tau}), \end{aligned} \tag{19}$$

where $\Psi_{m,1} = [(e^{\kappa_{m,1}\bar{\tau}_{m,1}})/2(1-\check{\tau}_{m,1})]h_{m,1}^2(x_{m,1})$.

By utilizing Assumption 3 and Young's inequality yields

$$p_{m,1}s_{m,1}g_{m,1} \le \frac{1}{2}p_{m,1}^2 s_{m,1}^2 + \sum_{l=1}^{M}\varpi_{m,l}\aleph_1^2(\bar{x}_{l,1}) \le \frac{p_{m,1}^2}{2}s_{m,1}^2 + 16\tanh^2\left(\frac{s_{m,1}}{\sigma_{m,1}}\right)\sum_{l=1}^{M}\varpi_{m,l}\aleph_1^2(\bar{x}_{m,1}) + \left(1 - 16\tanh^2\left(\frac{s_{m,1}}{\sigma_{m,1}}\right)\right)\sum_{l=1}^{M}\varpi_{m,l}\aleph_1^2(\bar{x}_{m,1}) + \sum_{l=1}^{M}\varpi_{m,l}(\aleph_1^2(\bar{x}_{l,1}) - \aleph_1^2(\bar{x}_{m,1})), \tag{20}$$

where $\varpi_{m,l} = (1/2)Mj_{m,l}^2$.

In light of Assumption 1 and Lemma 3 holds

$$p_{m,1}s_{m,1}\Delta_{m,1} \le p_{m,1} \mid s_{m,1} \mid \bar{\varphi}_{m,11}(\|x_{m,1}\|) + 0.2785\jmath_{m,11} + p_{m,1} \mid s_{m,1} \mid \varphi_{m,12}(\|\psi_i\|), \tag{21}$$

where $\jmath_{m,11} > 0$ denotes a constant and $\bar{\varphi}_{m,11}(\|x_{m,1}\|) = \varphi_{m,11}(\|x_{m,1}\|)\tanh\big((p_{m,1} \mid s_{m,1} \mid \varphi_{m,11}(x_{m,1}))/\jmath_{m,11}\big)$.

In view of Assumption 2 and Lemma 3, one obtains

$$p_{m,1} \mid s_{m,1} \mid \varphi_{m,12}(\|\psi_i\|) \le \frac{1}{2}\varphi_{m,12}^2(\vartheta_{m,1}^{-1}(2\bar{D}_m(t_0,t))) + \frac{p_{m,1}^2 s_{m,1}^2}{2} + p_{m,1}s_{m,1}\bar{\varphi}_{m,12}(x_{m,1},\lambda_m) + 0.2785\jmath_{m,12}, \tag{22}$$

where $\jmath_{m,12} > 0$ denotes a constant and $\bar{\varphi}_{m,12}(x_{m,1},\lambda_m) = \varphi_{m,12}(\vartheta_{m,1}^{-1}(2\lambda_m))\tanh\big((p_{m,1}s_{m,1}\varphi_{m,12}\big(\vartheta_{m,1}^{-1}(2\lambda_m))\big)/\jmath_{m,12}\big)$.

Calculating $\dot{V}_1$, one obtains

$$\dot{V}_1 \le \sum_{m=1}^{M}\Big[p_{m,1}s_{m,1}\big(s_{m,2} + \nu_{m,2} + \xi_{m,2} + \alpha_{m,1} + \frac{3}{2}p_{m,1}s_{m,1} + f_{m,1} - \frac{\dot{\ell}_m x_{m,1}}{\ell_m} - \frac{\dot{\nu}_{m,1}}{p_{m,1}}\Big) - \mu_{m,1}^{-1}\tilde{\Theta}_{m,1}\dot{\hat{\Theta}}_{m,1} - \frac{\bar{r}_{m,1}\lambda_m}{\varrho_{m0}} - \kappa_{m,1}\bar{V}_{m,1} + p_{m,1}s_{m,1}\varpi_{m,1} + 16\tanh^2\left(\frac{s_{m,1}}{\sigma_{m,1}}\right)\sum_{l=1}^{M}\varpi_{m,l}\aleph_1^2(\bar{x}_{m,1})\Big) + \frac{\bar{\pi}_{m0}(\|x_{m,1}(t)\|)}{\varrho_{m0}} + \left(1 - 16\tanh^2\left(\frac{s_{m,1}}{\sigma_{m,1}}\right)\right)\sum_{l=1}^{M}\varpi_{m,l}\aleph_1^2(\bar{x}_{m,1}) + \Psi_{m,1} + \sum_{l=1}^{M}\varpi_{m,l}(\aleph_1^2(\bar{x}_{l,1}) - \aleph_1^2(\bar{x}_{m,1})) + \chi_{m,1}\Big], \tag{23}$$

where $\varpi_{m,1} = \bar{\varphi}_{m,11}(\|x_{m,1}\|) + \bar{\varphi}_{m,12}(x_{m,1},\lambda_m)$ and $\chi_{m,1} = 0.2785\omega_{m,11} + 0.2785\omega_{m,12} + r_{m,2}/\varrho_{m0} + \frac{1}{2}\varphi_{m,12}^2(\vartheta_{m,1}^{-1}(2\bar{D}_m(t_0,t)))$.

The hyperbolic tangent function $16\tanh^2(s_{m,1}/\sigma_{m,1})$ is utilized to solve the $\Psi_{m,1}$, $\sum_{l=1}^{M}\varpi_{m,l}\aleph_i^2(\bar{x}_{l,1})$, and $(\bar{\pi}_{m0}(\|x_{m,1}(t)\|)/\varrho_{m0})$.

$$\dot{V}_1 \le \sum_{m=1}^{M}\Big[p_{m,1}s_{m,1}\big(s_{m,2} + \nu_{m,2} + \xi_{m,2} + \alpha_{m,1} + \frac{3}{2}p_{m,1}s_{m,1} + f_{m,1} - \frac{\dot{\ell}_m x_{m,1}}{\ell_m} - \frac{\dot{\nu}_{m,1}}{p_{m,1}} + \frac{16}{p_{m,1}s_{m,1}}\tanh^2\left(\frac{s_{m,1}}{\sigma_{m,1}}\right)G_{m,1}\big) - \mu_{m,1}^{-1}\tilde{\Theta}_{m,1}\dot{\hat{\Theta}}_{m,1} - \frac{\bar{r}_{m,1}\lambda_m}{\varrho_{m0}} + p_{m,1}s_{m,1}\varpi_{m,1} + \left(1 - 16\tanh^2\left(\frac{s_{m,1}}{\sigma_{m,1}}\right)\right)G_{m,1} - \kappa_{m,1}\bar{V}_{m,1} + \sum_{l=1}^{M}\varpi_{m,l}(\aleph_1^2(\bar{x}_{l,1}) - \aleph_1^2(\bar{x}_{m,1})) + \chi_{m,1}\Big], \tag{24}$$

where $G_{m,1} = \Psi_{m,1} + (\bar{\pi}_{m0}(\|x_{m,1}(t)\|))/\varrho_{m0} + \sum_{l=1}^{M}\varpi_{m,l}\aleph_i^2(\bar{x}_{m,1})$ and $\sigma_{m,1} > 0$ denotes a constant. □

Remark 1 Since $\lim_{s_{m,1}\to 0}[G_{m,1}/(p_{m,1}s_{m,1})] = \infty$, the lumped terms $G_{m,1}/(p_{m,1}s_{m,1})$ cannot be directly approximated by the RBFNNs. To tackle this obstacle, a hyperbolic tangent item $(16/p_m s_{m,1})\tanh^2(s_{m,1}/\sigma_{m,1}))G_{m,1}$ is used to prevent the singularity of the potential challenge. Meanwhile, two different cases will be further elaborated to handle the term $(1 - 16\tanh^2(s_{m,1}/\sigma_{m,1}))G_{m,1}$ in Sect. 3.3.

To further simplify the $\dot{V}_1$ in (24), the RBFNNs is employed to approximate the unknown item $F_{m,1}(\bar{z}_{m,1}) = f_{m,1} + (16/p_m s_{m,1})\tanh^2(s_{m,1}/\sigma_{m,1})G_{m,1} + \varpi_{m,1} + 2p_{m,1}s_{m,1}$, where the RBFNNs input vector $\bar{z}_{m,1} = [x_{m,1}, s_{m,1}, p_{m,1}, \lambda_1(t)]^{\mathrm{T}}$.

Thus, one has

$$F_{m,1}(\bar{z}_{m,1}) = W_{m,1}^{*T}S_{m,1}(\bar{z}_{m,1}) + \varepsilon_{m,1},$$

$$p_{m,1}s_{m,1}F_{m,1}(\bar{z}_{m,1}) \le \frac{p_{m,1}^2 s_{m,1}^2}{2a_{m,1}^2}\Theta_{m,1}S_{m,1}^{\mathrm{T}}(\cdot)S_{m,1}(\cdot) + \frac{a_{m,1}^2}{2} + \frac{1}{2}p_{m,1}^2 s_{m,1}^2 + \frac{\varepsilon_{m,1}^{*2}}{2}, \tag{25}$$

where $\varepsilon_{m,1}$ is the approximation error with $\mid \varepsilon_{m,1} \mid \le \varepsilon_{m,1}^*$.

Substituting (11), (12), (15), and (25) into (24) becomes

$$\dot{V}_1 \le \sum_{m=1}^{M}\Bigg[-c_{m,1}s_{m,1}^2 + p_{m,1}s_{m,1}s_{m,2} + \rho_{m,1}\tilde{\Theta}_{m,1}\hat{\Theta}_{m,1} - \frac{\bar{r}_{m,1}\lambda_m}{\varrho_{m0}} + \left(1 - 16\tanh^2\left(\frac{s_{m,1}}{\sigma_{m,1}}\right)\right)G_{m,1} - \kappa_{m,1}\bar{V}_{m,1} + \chi_{m,1} + \frac{\varepsilon_{m,1}^{*2}}{2} + \frac{a_{m,1}^2}{2} + \sum_{l=1}^{M}\bar{\varpi}_{m,l}(\aleph_1^2(\bar{x}_{l,1}) - \aleph_1^2(\bar{x}_{m,1}))\Bigg]. \tag{26}$$

Step m, i. From (10) and (11), it deduces that

$$\dot{s}_{m,i} = s_{m,i+1} + v_{m,i+1} + \xi_{m,i+1} + \alpha_{m,i} + f_{m,i} + \Delta_{m,i} + g_{m,i} + h_{m,i}(x_{m,i\tau}) - \dot{\zeta}_{m,i} - \dot{v}_{m,i}. \tag{27}$$

By utilizing Assumption 3 and Young's inequality holds

$$s_{m,i}g_{m,i} \le \frac{1}{2}s_{m,i}^2 + 16\tanh^2\left(\frac{s_{m,i}}{\sigma_{m,i}}\right)\sum_{l=1}^{M}\bar{\varpi}_{m,l}\aleph_i^2(\bar{x}_{m,i}) + \left(1 - 16\tanh^2\left(\frac{s_{m,i}}{\sigma_{m,i}}\right)\right)\sum_{l=1}^{M}\bar{\varpi}_{m,l}\aleph_i^2(\bar{x}_{m,i}) + \sum_{l=1}^{M}\bar{\varpi}_{m,l}(\aleph_i^2(\bar{x}_{l,i}) - \aleph_i^2(\bar{x}_{m,i})). \tag{28}$$

Select the following Lyapunov function candidate:

$$V_i = V_{i-1} + \sum_{m=1}^{M}\left[\frac{1}{2}s_{m,i}^2 + \frac{1}{2\mu_{m,i}}\tilde{\Theta}_{m,i}^2 + \bar{V}_{m,i}\right],$$

where $\kappa_{m,i} > 0$ denotes a constant and $\bar{V}_{m,i} = (e^{\kappa_{m,i}\bar{\tau}_{m,i}}/2(1-\check{\tau}_{m,i}))\int_{t-\tau_{m,i}(t)}^{t} e^{-\kappa_{m,i}(t-s)}h_{m,i}^2(x_{m,i}(s))ds$.

Through calculation, one has

$$\dot{\bar{V}}_{m,i} \le -\kappa_{m,i}\bar{V}_{m,i} + \Psi_{m,i} - \frac{1}{2}h_{m,i}^2(x_{m,i\tau}),$$
$$s_{m,i}h_{m,i}(x_{m,i\tau}) \le \frac{1}{2}s_{m,i}^2 + \frac{1}{2}h_{m,i}^2(x_{m,i\tau}), \tag{29}$$

where $\Psi_{m,i} = (e^{\kappa_{m,i}\bar{\tau}_{m,i}}/2(1-\check{\tau}_{m,i}))h_{m,i}^2(x_{m,i})$.

Similar to (21) and (22) yields

$$s_{m,i}\Delta_{m,i} \le |\, s_{m,i}\,|\,\varphi_{m,i1}(\|\bar{x}_{m,i}\|)\tanh\left(\frac{|\, s_{m,i}\,|\,\varphi_{m,i1}(\bar{x}_{m,i})}{\jmath_{m,i1}}\right) + 0.2785\jmath_{m,i1} + |\, s_{m,i}\,|\,\varphi_{m,i2}(\|\psi_i\|), \tag{30}$$

where $\jmath_{m,i1} > 0$ denotes a constant.

$$|\, s_{m,i}\,|\,\varphi_{m,i2}(\|\psi_i\|) \le s_{m,i}\bar{\varphi}_{m,i2}(\bar{x}_{m,i},\lambda_m) + 0.2785\jmath_{m,i2} + \frac{s_{m,i}^2}{2} + \frac{1}{2}\varphi_{m,i2}^2(\vartheta_{m,i}^{-1}(2\bar{D}_m(t_0,t))), \tag{31}$$

where $\jmath_{m,i2} > 0$ denotes a constant and $\bar{\varphi}_{m,i2}(\bar{x}_{m,i},\lambda_m) = \varphi_{m,i2}(\vartheta_{m,i}^{-1}(2\lambda_m))\tanh((s_{m,i}\varphi_{m,i2}(\vartheta_{m,i}^{-1}(2\lambda_m)))/\jmath_{m,i2})$.

The time derivative of V_i can be obtained

$$\dot{V}_i \le \dot{V}_{i-1} + \sum_{m=1}^{M}\Bigg[s_{m,i}\Bigg(s_{m,i+1} + v_{m,i+1} + \frac{3}{2}s_{m,i} + \xi_{m,i+1} + \alpha_{m,i} - \dot{\zeta}_{m,i} + \frac{16}{s_{m,i}}\tanh^2\left(\frac{s_{m,i}}{\sigma_{m,i}}\right)\sum_{l=1}^{M}\bar{\varpi}_{m,l}\aleph_i^2(\bar{x}_{m,i}) + f_{m,i} - \dot{v}_{m,i}\Bigg) - \kappa_{m,i}\bar{V}_{m,i} - \mu_{m,i}^{-1}\tilde{\Theta}_{m,i}\dot{\hat{\Theta}}_{m,i} + \left(1 - 16\tanh^2\left(\frac{s_{m,i}}{\sigma_{m,i}}\right)\right)\sum_{l=1}^{M}\bar{\varpi}_{m,l}\aleph_i^2(\bar{x}_{m,i}) + s_{m,i}\varpi_{m,i} + \Psi_{m,i} + \sum_{l=1}^{M}\bar{\varpi}_{m,l}(\aleph_i^2(\bar{x}_{l,i}) - \aleph_i^2(\bar{x}_{m,i})) + \chi_{m,i}\Bigg], \tag{32}$$

where $\varpi_{m,i} = \varphi_{m,i1}(\|\bar{x}_{m,i}\|)\tanh((|\, s_{m,i}\,|\,\varphi_{m,i1}(\bar{x}_{m,i}))/\jmath_{m,i1}) + \bar{\varphi}_{m,i2}(\bar{x}_{m,i},\lambda_m)$ and $\chi_{m,i} = \frac{1}{2}\varphi_{m,i2}^2(\vartheta_{m,i}^{-1}(2\bar{D}_m(t_0,t))) + 0.2785\jmath_{m,i1} + 0.2785\jmath_{m,i2}$.

By applying the hyperbolic tangent function, $\dot{V}_i$ becomes

$$\dot{V}_i \le \dot{V}_{i-1} + \sum_{m=1}^{M}\Bigg[s_{m,i}\Bigg(s_{m,i+1} + v_{m,i+1} + \xi_{m,i+1} + \frac{3}{2}s_{m,i} - \dot{\zeta}_{m,i} - \dot{v}_{m,i} + f_{m,i} + \alpha_{m,i} + \frac{16}{s_{m,i}}\tanh^2\left(\frac{s_{m,i}}{\sigma_{m,i}}\right)G_{m,i}\Bigg) - \mu_{m,i}^{-1}\tilde{\Theta}_{m,i}\dot{\hat{\Theta}}_{m,i} + s_{m,i}\varpi_{m,i} - \kappa_{m,i}\bar{V}_{m,1} + \left(1 - 16\tanh^2\left(\frac{s_{m,i}}{\sigma_{m,i}}\right)\right)G_{m,i} + \sum_{l=1}^{M}\bar{\varpi}_{m,l}(\aleph_i^2(\bar{x}_{l,i}) - \aleph_i^2(\bar{x}_{m,i})) + \chi_{m,i}\Bigg], \tag{33}$$

where $G_{m,i} = \Psi_{m,i} + \sum_{l=1}^{M}\bar{\varpi}_{m,l}\aleph_i^2(\bar{x}_{m,i})$.

The RBFNNs is utilized to approximate the unknown item $F_{m,i}(\bar{z}_{m,i}) = f_{m,i} + (16/s_{m,i})\tanh^2(s_{m,i}/\sigma_{m,i})G_{m,i} + \varpi_{m,i} - \dot{\zeta}_{m,i} + 2s_{m,i}$ in (33), where the RBFNNs input vector $\bar{z}_{m,i} = [x_{m,i}, s_{m,i}, \lambda_i(t), \dot{\zeta}_{m,i}]^{\mathrm{T}}$. Therefore, one obtains

$$F_{m,i}(\bar{z}_{m,i}) = W_{m,i}^{*T}S_{m,i}(\bar{z}_{m,i}) + \varepsilon_{m,i},$$
$$s_{m,i}F_{m,i}(\bar{z}_{m,i}) \le \frac{s_{m,i}^2}{2a_{m,i}^2}\Theta_{m,i}S_{m,i}^{\mathrm{T}}(\cdot)S_{m,i}(\cdot) + \frac{a_{m,i}^2}{2} + \frac{1}{2}s_{m,i}^2 + \frac{\varepsilon_{m,i}^{*2}}{2}, \tag{34}$$

where $\varepsilon_{m,i}$ is the approximation error with $|\, \varepsilon_{m,i}\,| \le \varepsilon_{m,i}^*$.

Substituting (11), (13), (16), and (34) into (33) yields

$$\begin{aligned}\dot{V}_i \le \sum_{m=1}^{M}\Bigg[&-\sum_{k=1}^{i} c_{m,k}s_{m,k}^2 + s_{m,i}s_{m,i+1} + \sum_{k=1}^{i}\rho_{m,k}\tilde{\Theta}_{m,k}\hat{\Theta}_{m,k}\\ &-\sum_{k=1}^{i}\kappa_{m,k}\bar{V}_{m,k}\\ &+\sum_{k=1}^{i}\left(1-16\tanh^2\left(\frac{s_{m,k}}{\sigma_{m,k}}\right)\right)G_{m,k} - \frac{\bar{r}_{m,1}\lambda_m}{\varrho_{m0}}\\ &+\sum_{k=1}^{i}\frac{\varepsilon_{m,k}^{*2}}{2} + \sum_{k=1}^{i}\frac{a_{m,k}^2}{2}\\ &+\sum_{k=1}^{i}\sum_{l=1}^{M}\bar{\varpi}_{m,l}(\aleph_k^2(\bar{x}_{l,k}) - \aleph_k^2(\bar{x}_{m,k})) + \sum_{k=1}^{i}\chi_{m,k}\Bigg].\end{aligned} \tag{35}$$

Step m, n_m. In industrial process, the existence of actuator saturation nonlinearity will affect the system stability. Therefore, the following saturation function is considered:

$$u_m = \mathrm{sat}(\bar{u}_m) = \begin{cases} \mathrm{sign}(\bar{u}_m)u_m^{\mathrm{Max}}, & |\bar{u}_m| \ge u_m^{\mathrm{Max}},\\ \bar{u}_m, & |\bar{u}_m| < u_m^{\mathrm{Max}},\end{cases}$$

where u_m^{Max} is the bound of u_m and $\bar{u}_m$ is the input of the following saturation nonlinearity:

$$\bar{b}_m(\bar{u}_m) = u_m^{\mathrm{Max}} * \frac{e^{\frac{\bar{u}_m}{u_m^{\mathrm{Max}}}} - e^{-\frac{\bar{u}_m}{u_m^{\mathrm{Max}}}}}{e^{\frac{\bar{u}_m}{u_m^{\mathrm{Max}}}} + e^{-\frac{\bar{u}_m}{u_m^{\mathrm{Max}}}}}.$$

Meanwhile the quantized parameters satisfy $(1-\bar{\kappa}_m)u_m^{\min}/(\bar{\kappa}_m + \hbar_m) \ge u_m^{\mathrm{Max}}$. Referring to [40], $\mathrm{sat}(\bar{u}_m)$ becomes

$$u_m = \mathrm{sat}(\bar{u}_m) = \bar{b}_m(\bar{u}_m) + \bar{\varrho}_m(\bar{u}_m), \tag{36}$$

where $|\bar{\varrho}(\bar{u}_m)| = |\mathrm{sat}(\bar{u}_m)) - \bar{b}_m(\bar{u}_m)| \le u_m^{\mathrm{Max}}(1-\tanh(1)) = \underline{\varrho}_m$.

According to the mean-value theorem, $\bar{b}_m(\bar{u}_m)$ can be expressed as:

$$\bar{b}_m(\bar{u}_m) = \bar{b}_m(\bar{u}_{m0}) + \frac{\partial \bar{b}_m(\cdot)}{\partial \bar{u}_m}|_{\bar{u}_m=\bar{u}_m^{c_m}}(\bar{u}_m - \bar{u}_{m0}), \tag{37}$$

where $\bar{u}_m^{c_m} = c_m\bar{u}_m + (1-c_m)\bar{u}_{m0}$ and $0<c_m<1$.

Let $\bar{u}_{m0} = 0$, (37) becomes

$$\bar{b}_m(\bar{u}_m) = \frac{\partial \bar{b}_m(\cdot)}{\partial \bar{u}_m}|_{\bar{u}_m=\bar{u}_m^{c_m}}\bar{u}_m = \zeta_{m0}(\bar{u}_m^{c_m})\bar{u}_m. \tag{38}$$

For the positive constants $\underline{\zeta}_{m0}$ and $\bar{\zeta}_{m0}$, the expression $\underline{\zeta}_{m0} < \zeta_{m0}(\bar{u}_m^{c_m}) < \bar{\zeta}_{m0}$ holds. Thus, (36) becomes

$$u_m = \mathrm{sat}(\bar{u}_m) = \zeta_{m0}(\bar{u}_m^{c_m})\bar{u}_m + \bar{\varrho}_m(\bar{u}_m). \tag{39}$$

According to (9)–(11) and (39), $\dot{s}_{m,n_m}$ can be expressed as:

$$\begin{aligned}\dot{s}_{m,n_m} =\ &(1-\bar{\kappa}_m)\zeta_{m0}\bar{u}_m + (1-\bar{\kappa}_m)\bar{\varrho}_m + \bar{\kappa}_m\bar{\varsigma}_m\\ &+ f_{m,n_m} + \Delta_{m,n_m}\\ &+ h_{m,n_m}(x_{m,n_m\tau}) + g_{m,n_m} - \dot{\zeta}_{m,n_m} - \dot{v}_{m,n_m}.\end{aligned} \tag{40}$$

Let us construct the Lyapunov function candidate as $V_{n_m} = V_{n_m-1} + \sum_{m=1}^{M}\left[\frac{1}{2}s_{m,n_m}^2 + \frac{1}{2\mu_{m,n_m}}\tilde{\Theta}_{m,n_m}^2 + \bar{V}_{m,n_m}\right]$.

By utilizing Young's inequality, one has

$$s_{m,n_m}(1-\bar{\kappa}_m)\bar{\varrho}_m \le \frac{1}{2}s_{m,n_m}^2 + \frac{1}{2}(1-\bar{\kappa}_m)^2\underline{\varrho}_m^2. \tag{41}$$

Then, it can be deduced that

$$\begin{aligned}\dot{V}_{n_m} \le \dot{V}_{n_m-1} + \sum_{m=1}^{M}\Bigg[&s_{m,n_m}((1-\bar{\kappa}_m)\zeta_{m0}\bar{u}_m + 2s_{m,n_m} + f_{m,n_m} - \dot{\zeta}_{m,n_m}\\ &+\frac{16}{s_{m,n_m}}\tanh^2\left(\frac{s_{m,n_m}}{\sigma_{m,n_m}}\right)\sum_{l=1}^{M}\bar{\varpi}_{m,l}\aleph_{n_m}^2(\bar{x}_{m,n_m}) - \dot{v}_{m,n_m}\\ &+\left(1-16\tanh^2\left(\frac{s_{m,n_m}}{\sigma_{m,n_m}}\right)\right)\sum_{l=1}^{M}\bar{\varpi}_{m,l}\aleph_{n_m}^2(\bar{x}_{m,n_m})) + \bar{\kappa}_m\bar{\varsigma}_m\\ &-\kappa_{m,n_m}\bar{V}_{m,n_m} + s_{m,n_m}\varpi_{m,n_m} - \mu_{m,n_m}^{-1}\tilde{\Theta}_{m,n_m}\dot{\hat{\Theta}}_{m,n_m}\\ &+\Psi_{m,n_m} + \sum_{l=1}^{M}\bar{\varpi}_{m,l}(\aleph_{n_m}^2(\bar{x}_{l,n_m}) - \aleph_{n_m}^2(\bar{x}_{m,n_m})) + \chi_{m,n_m}\Bigg],\end{aligned} \tag{42}$$

where

$$\begin{aligned}\Psi_{m,n_m} &= [e^{\kappa_{m,n_m}\bar{\tau}_{m,n_m}}h_{m,n_m}^2(x_{m,n_m})/2(1-\check{\tau}_{m,n_m})],\\ \varpi_{m,n_m} &= \varphi_{m,n_m1}(\|\bar{x}_{m,n_m}\|)\tanh((|s_{m,n_m}|\varphi_{m,n_m1}(\bar{x}_{m,n_m}))/\jmath_{m,n_m1})\\ &\quad + \bar{\varphi}_{m,n_m2}(\bar{x}_{m,n_m},\lambda_m),\\ \chi_{m,n_m} &= 0.2785\jmath_{m,n_m1} + 0.5\varphi_{m,n_m2}^2(\vartheta_{m,n_m}^{-1}(2\bar{D}_m(t_0,t)))\\ &\quad + 0.2785\jmath_{m,n_m2} + 0.5(1-\bar{\kappa}_m)^2\underline{\varrho}_m^2.\end{aligned}$$

Define $G_{m,n_m} = \Psi_{m,n_m} + \sum_{l=1}^{M}\bar{\varpi}_{m,l}\aleph_{n_m}^2(\bar{x}_{m,n_m})$ yields

$$\begin{aligned}\dot{V}_{n_m} \le \dot{V}_{n_m-1} + \sum_{m=1}^{M}\Bigg[&s_{m,n_m}\Bigg((1-\bar{\kappa}_m)\zeta_{m0}\bar{u}_m + \bar{\kappa}_m\bar{\varsigma}_m + f_{m,n_m} - \dot{\zeta}_{m,n_m}\\ &+\frac{16}{s_{m,n_m}}\tanh^2\left(\frac{s_{m,n_m}}{\sigma_{m,n_m}}\right)G_{m,n_m} + \varpi_{m,n_m} - \dot{v}_{m,n_m} + 2s_{m,n_m}\Bigg)\\ &-\mu_{m,n_m}^{-1}\tilde{\Theta}_{m,n_m}\dot{\hat{\Theta}}_{m,n_m} + \left(1-16\tanh^2\left(\frac{s_{m,n_m}}{\sigma_{m,n_m}}\right)\right)G_{m,n_m}\\ &+\chi_{m,n_m} - \kappa_{m,n_m}\bar{V}_{m,n_m} + \sum_{l=1}^{M}\bar{\varpi}_{m,l}(\aleph_{n_m}^2(\bar{x}_{l,n_m})\\ &-\aleph_{n_m}^2(\bar{x}_{m,n_m}))\Bigg].\end{aligned} \tag{43}$$

The RBFNNs is employed to approximate the unknown function

$$F_{m,n_m}(\bar{z}_{m,n_m}) = f_{m,n_m} + (16/s_{m,n_m})\tanh^2(s_{m,n_m}/\sigma_{m,n_m})G_{m,n_m} + \varpi_{m,n_m} - \dot{\zeta}_{m,n_m} + 2.5s_{m,n_m}$$

in (43), where the RBFNNs input vector $\bar{z}_{m,n_m} = [x_{m,n_m}, s_{m,n_m}, \lambda_{n_m}(t), \dot{\zeta}_{m,n_m}]^{\mathrm{T}}$. Therefore, one obtains

$$\begin{aligned} &F_{m,n_m}(\bar{z}_{m,n_m}) = W^{*T}_{m,n_m} S_{m,i}(\bar{z}_{m,n_m}) + \varepsilon_{m,n_m}, \\ &s_{m,n_m}F_{m,n_m}(\bar{z}_{m,n_m}) \le \frac{s^2_{m,n_m}}{2a^2_{m,n_m}}\Theta_{m,n_m}S^{\mathrm{T}}_{m,n_m}(\cdot)S_{m,n_m}(\cdot) \\ &\quad + \frac{a^2_{m,n_m}}{2} + \frac{1}{2}s^2_{m,n_m} + \frac{\varepsilon^{*2}_{m,n_m}}{2}. \end{aligned} \tag{44}$$

where ε_{m,n_m} is the approximation error with $|\varepsilon_{m,n_m}| \le \varepsilon^*_{m,n_m}$.

Meanwhile, the self-triggered scheme is developed as follows:

$$\begin{aligned} &\bar{u}_m(t) = v_m(t_k), \ \forall t \in [t_k, t_{k+1}), \\ &t_{k+1} = t_k + \frac{\Lambda_m |\bar{u}_m(t)| + E_m}{\max\{L_m, |\dot{v}_m(t)|\}}, \end{aligned} \tag{45}$$

where $t_k, t_{k+1} \in Z^+; 0 < \Lambda_m < 1$, E_m and L_m are positive constant. $\Lambda_m |\bar{u}_m(t)| + E_m$ denotes control signal interval between two successive triggered instants; L_m and $|\dot{v}_m(t)|$ are change rates of control signal interval.

When the conditions of (45) are satisfied, $\bar{u}_m(t) = v_m(t_k)$ will be used to the control plant in (1). The next trigger point t_{k+1} will be obtained, and control signal $\bar{u}_m(t)$ holds as a constant $v_m(t_k)$ in the period interval $[t_k, t_{k+1})$.

$v_m(t_k)$ is constructed as follows:

$$\begin{aligned} v_m = &-(1+\Lambda_m)\left(\alpha_{m,n_m}\tanh\left(\frac{s_{m,n_m}\alpha_{m,n_m}}{\jmath_m}\right)\right. \\ &\left. + \bar{E}_m\tanh\left(\frac{s_{m,n_m}\bar{E}_m}{\jmath_m}\right)\right), \end{aligned} \tag{46}$$

where $\jmath_m > 0$ and $\bar{E}_m > E_m/(1-\Lambda_m)$.

From (45), it has $|\bar{u}_m(t_{k+1}) - u_m(t)| \le \Lambda_m |\bar{u}_m(t)| + E_m$. There exist the continuous time-varying parameters $\theta_{m,1}, \theta_{m,2}$ satisfying $\theta_{m,1}(t_k) = \theta_{m,2}(t_k) = 0, \theta_{m,1}(t_{k+1}) = \theta_{m,2}(t_{k+1}) = \pm 1$ and $|\theta_{m,1}| \le 1, |\theta_{m,2}| \le 1, \forall t \in [t_k, t_{k+1})$,

$$\bar{u}_m = \frac{v_m - \theta_{m,2}E_m}{1 + \theta_{m,1}\Lambda_m}. \tag{47}$$

Therefore, $\dot{V}_{n_m}$ can be expressed as:

$$\begin{aligned} \dot{V}_{n_m} \le \dot{V}_{n_m-1} + \sum_{m=1}^{M}\Bigg[&s_{m,n_m}\Bigg((1-\bar{\kappa}_m)\zeta_{m0}\frac{v_m - \theta_{m,2}E_m}{1+\theta_{m,1}\Lambda_m} \\ &+ \bar{\kappa}_m\bar{\varsigma}_m - \dot{v}_{m,n_m} \\ &+ \frac{s_{m,n_m}}{2a^2_{m,n_m}}\Theta_{m,n_m}S^{\mathrm{T}}_{m,n_m}S_{m,n_m}\Bigg) \\ &- \mu^{-1}_{m,n_m}\tilde{\Theta}_{m,n_m}\dot{\hat{\Theta}}_{m,n_m} + \frac{a^2_{m,n_m}}{2} \\ &- \kappa_{m,n_m}\bar{V}_{m,n_m} + \left(1 - 16\tanh^2\left(\frac{s_{m,n_m}}{\sigma_{m,n_m}}\right)\right)G_{m,n_m} \\ &+ \frac{\varepsilon^{*2}_{m,n_m}}{2} \\ &+ \sum_{l=1}^{M}\bar{\varpi}_{m,l}(\aleph^2_{n_m}(\bar{x}_{l,n_m}) - \aleph^2_{n_m}(\bar{x}_{m,n_m})) + \chi_{m,n_m}\Bigg]. \end{aligned} \tag{48}$$

On the basis of (46) and Lemma 3, it has $s_{m,n_m}v_m < 0$. In light of $0 < [(s_{m,n_m}v_m)/(1+\theta_{m,1}\Lambda_m)] < [(s_{m,n_m}v_m)/(1+\Lambda_m)]$ and $-[(s_{m,n_m}\theta_{m,2}E_m)/(1+\theta_{m,1}\Lambda_m)] \le |s_{m,n_m}E_m/1 - \Lambda_m| \le |s_{m,n_m}\bar{E}_m|$, the following inequality holds

$$\begin{aligned} &s_{m,n_m}(1-\bar{\kappa}_m)\zeta_{m0}\left(\frac{v_m - \theta_{m,2}E_m}{1+\theta_{m,1}\Lambda_m} - \alpha_{m,n_m}\right) \\ &\le \frac{s_{m,n_m}(1-\bar{\kappa}_m)\zeta_{m0}v_m}{1+\Lambda_m} + |s_{m,n_m}(1-\bar{\kappa}_m)\zeta_{m0}\bar{E}_m| \\ &\quad - s_{m,n_m}(1-\bar{\kappa}_m)\zeta_{m0}\alpha_{m,n_m} \\ &\le 0.557\jmath_m(1-\bar{\kappa}_m)\zeta_{m0}. \end{aligned} \tag{49}$$

Since $\tilde{\Theta}_{m,i}\hat{\Theta}_{m,i} \le -(\tilde{\Theta}^2_{m,i}/2) + (\Theta^2_{m,i}/2)$ and invoking (11), (14), (48) and (49) results in

$$\begin{aligned} \dot{V}_{n_m} \le \sum_{m=1}^{M}\Bigg[&-\sum_{k=1}^{n_m}c_{m,k}s^2_{m,k} - \sum_{k=1}^{n_m}\frac{\rho_{m,k}}{2}\tilde{\Theta}^2_{m,k} - \frac{\bar{r}_{m,1}\lambda_m}{\varrho_{m0}} \\ &- \sum_{k=1}^{n_m}\kappa_{m,k}\bar{V}_{m,k} \\ &+ \sum_{k=1}^{n_m}\left(1 - 16\tanh^2\left(\frac{s_{m,k}}{\sigma_{m,k}}\right)\right)G_{m,k} - (1-\bar{\kappa}_m)s_{m,n_m}u^{\min}_m \\ &+ s_{m,n_m}\bar{\kappa}_m\bar{\varsigma}_m + \bar{\chi}_m + \sum_{k=1}^{n_m}\sum_{l=1}^{M}\bar{\varpi}_{m,l}(\aleph^2_k(\bar{x}_{l,k}) - \aleph^2_k(\bar{x}_{m,k}))\Bigg], \end{aligned} \tag{50}$$

where $\bar{\chi}_m = \sum_{k=1}^{n_m}\chi_{m,k} + \sum_{k=1}^{n_m}(\rho_{m,k}/2)\Theta^2_{m,k} + \sum_{k=1}^{n_m}(a^2_{m,k}/2) + \sum_{k=1}^{n_m}(\varepsilon^{*2}_{m,k}/2) + 0.557\jmath_m(1-\bar{\kappa}_m)\zeta_{m0}$.

From the analysis in [16, 41], the Lyapunov function is designed as $V = \bar{\delta}_m V_{n_m}$, where $\bar{\delta}_m > 0$ refers to the cofactor of the mth diagonal element by instead of $r_{m,l}$ with $\bar{\varpi}_{m,l}$. Thus, (50) becomes

$$\dot{V}_{n_m} \le \sum_{m=1}^{M} \bar{\delta}_m \Bigg[-\sum_{k=1}^{n_m} c_{m,k} s_{m,k}^2 - \sum_{k=1}^{n_m} \frac{\rho_{m,k}}{2} \tilde{\Theta}_{m,k}^2 - \frac{\bar{r}_{m,1}\lambda_m}{\varrho_{m0}} - \sum_{k=1}^{n_m} \kappa_{m,k} \bar{V}_{m,k} + \sum_{k=1}^{n_m} \left(1 - 16\tanh^2\left(\frac{s_{m,k}}{\sigma_{m,k}}\right)\right) G_{m,k} - (1-\bar{\kappa}_m) s_{m,n_m} u_m^{\min} + s_{m,n_m}\bar{\kappa}_m\bar{\varsigma}_m + \bar{\gamma}_m + \sum_{k=1}^{n_m}\sum_{l=1}^{M} \bar{\varpi}_{m,l}(\aleph_k^2(\bar{x}_{l,k}) - \aleph_k^2(\bar{x}_{m,k})) \Bigg]. \tag{51}$$

In light of [4], $\sum_{m=1}^{M}\sum_{k=1}^{n_m}\sum_{l=1}^{M} \bar{\delta}_m \bar{\varpi}_{m,l}(\aleph_k^2(\bar{x}_{l,k}) - \aleph_k^2(\bar{x}_{m,k})) = 0$ holds. Therefore, (51) arrives at

$$\dot{V} \le \sum_{m=1}^{M} \bar{\delta}_m \Bigg[-\sum_{k=1}^{n_m} c_{m,k} s_{m,k}^2 - \sum_{k=1}^{n_m} \frac{\rho_{m,k}}{2} \tilde{\Theta}_{m,k}^2 - \frac{\bar{r}_{m,1}\lambda_m}{\varrho_{m0}} + \sum_{k=1}^{n_m} \left(1 - 16\tanh^2\left(\frac{s_{m,k}}{\sigma_{m,k}}\right)\right) G_{m,k} - (1-\bar{\kappa}_m) s_{m,n_m} u_m^{\min} + s_{m,n_m}\bar{\kappa}_m\bar{\varsigma}_m - \sum_{k=1}^{n_m} \kappa_{m,k}\bar{V}_{m,k} + \bar{\gamma}_m \Bigg]. \tag{52}$$

To this end, the adaptive self-triggered neural control scheme was preliminary accomplished. The results are summarized in the following Theorem 1.

3.3 Stability analysis

Theorem 1 *Let us consider the interconnected nonlinear time-delay system in (1), under Assumptions 1–3, the error compensation signals in (11), the virtual control functions in (12)–(14), the adaptive updating law in (15)–(16), then the decentralized-based adaptive quantized control algorithm guarantees the following features*:

- *The system output was confined to a small adjustable region in finite time.*
- *All the signals of the CLS remain SGUUB.*
- *The Zeno phenomenon was ruled out.*

Proof Let us select the Lyapunov function $\bar{V}_v = \sum_{m=1}^{M}\sum_{i=1}^{n_m} \frac{1}{2} v_{m,i}^2$ to prove the boundedness of $v_{m,i}$.

$$\begin{aligned}\dot{\bar{V}}_v &= \sum_{m=1}^{M} \Big[-c_{m,1} v_{m,1}^2 + p_{m,1} v_{m,1} v_{m,2} + p_{m,1} v_{m,1}\xi_{m,2} - c_{m,2} v_{m,2}^2 - p_{m,1} v_{m,1} v_{m,2} + v_{m,2} v_{m,3} + v_{m,2}\xi_{m,3} + \cdots - c_{m,n_m} v_{m,n_m}^2 - p_{m,n_m-1} v_{m,n_m-1} v_{m,n_m} \Big] \\ &= \sum_{m=1}^{M} \Bigg[-\sum_{l=1}^{n_m} c_{m,l} v_{m,l}^2 + \sum_{l=1}^{n_m-1} p_l v_{m,l}\xi_{m,l+1} \Bigg],\end{aligned} \tag{53}$$

where $p_l = \max\{p_{m,1}, 1\}$.

From [27], one has $\xi_{m,l+1} = | \zeta_{m,l+1} - \alpha_{m,l} | \le \Delta_{m,l}$ $(l = 1, \cdots, n_m - 1)$ and define $D_1 = \min\{(c_{m,1} - p_{m,1}^2/2),\ (c_{m,2} - 1/2), \ldots, (c_{m,n_m} - 1/2)\}$ and $D_2 = \frac{1}{2}\Delta_{m,l}^2$. Thus, (53) yields

$$\begin{aligned}\dot{\bar{V}}_v &\le \sum_{m=1}^{M} \Bigg[-\sum_{l=1}^{n_m} c_{m,l} v_{m,l}^2 + \sum_{l=1}^{n_m} p_l \Delta_{m,l} \mid v_{m,l} \mid \Bigg] \\ &\le -D_1 \bar{V}_v + D_2.\end{aligned} \tag{54}$$

Therefore, the boundness of $v_{m,i}$ can be obtained. This completes the proof. □

Let $A = \min \bar{\delta}_m \{2c_{m,k}, \rho_{m,k}\mu_{m,k}, \bar{r}_{m,1}, \kappa_{m,k}\}$ and $\chi_{n_m} = \sum_{m=1}^{M} \bar{\delta}_m \bar{\chi}_m$, (52) is further simplified as:

$$\begin{aligned}\dot{V} \le & -AV + \chi_{n_m} + \sum_{m=1}^{M}\sum_{k=1}^{n_m} \bar{\delta}_m \left(1 - 16\tanh^2\left(\frac{s_{m,k}}{\sigma_{m,k}}\right)\right) G_{m,k} \\ & + \sum_{m=1}^{M} (s_{m,n_m}\bar{\kappa}_m\bar{\varsigma}_m - (1-\bar{\kappa}_m) s_{m,n_m} u_m^{\min}).\end{aligned} \tag{55}$$

Firstly, by using Lemma 1, let us discuss the following two cases about $\sum_{m=1}^{M}(s_{m,n_m}\bar{\kappa}_m\bar{\varsigma}_m - (1-\bar{\kappa}_m) s_{m,n_m} u_m^{\min})$.

Case I: $u_m^{\min} \le u_m^{\mathrm{Max}}$, there exist two probabilities, i.e.,

(a): $| u_m | \le u_m^{\min}$,based on Lemma 1 with $| \bar{\varsigma}_m(t) | \le (1-\bar{\kappa}_m) u_m^{\min}/\bar{\kappa}_m$, it can be obtained

$$\dot{V} \le -AV + \sum_{m=1}^{M}\sum_{k=1}^{n_m} \bar{\delta}_m \left(1 - 16\tanh^2\left(\frac{s_{m,k}}{\sigma_{m,k}}\right)\right) G_{m,k} + \chi_{n_m}. \tag{56}$$

(b): $| u_m | \ge u_m^{\min}$, based on Lemma 1 and $| \bar{\varsigma}_m(t) | \le (\bar{\kappa}_m + \bar{\hbar}_m) | u_m | /\bar{\kappa}_m$, one has

$$\begin{aligned}\dot{V} \le & -AV + \chi_{n_m} + \sum_{m=1}^{M}\sum_{k=1}^{n_m} \bar{\delta}_m \left(1 - 16\tanh^2\left(\frac{s_{m,k}}{\sigma_{m,k}}\right)\right) G_{m,k} \\ & + \sum_{m=1}^{M} \big(s_{m,n_m}(\bar{\kappa}_m + \bar{\hbar}_m) \mid u_m \mid -(1-\bar{\kappa}_m) s_{m,n_m} u_m^{\min}\big).\end{aligned} \tag{57}$$

Since $(1-\bar{\kappa}_m) u_m^{\min}/(\bar{\kappa}_m + \bar{\hbar}_m) \ge u_m^{\mathrm{Max}}$, then we can obtain $| u_m | \le u_m^{\mathrm{Max}} \le (1-\bar{\kappa}_m) u_m^{\min}/(\bar{\kappa}_m + \bar{\hbar}_m)$. By invoking (57), the similar results with the form in (56) can be derived.

Case II $u_m^{\min} \ge u_m^{\mathrm{Max}}$, then $| u_m | \le u_m^{\min}$. The similar result can be derived by referring to **(a)** in **Case I**.

In a nutshell, by combining with the **Case I** and II, the inequality (56) can be obtained accordingly.

Next, let us discuss the sign of $\sum_{m=1}^{M}\sum_{k=1}^{n_m}\bar{\delta}_m(1-16\tanh^2(s_{m,k}/\sigma_{m,k}))G_{m,k}$, two cases exist as follows:

Case A $s_{m,k}\in\Omega_{m_k}=\{s_{m,k}\,||\,s_{m,k}\,|<0.2554m_k\}$ for $1\le m\le M$ and $1\le k\le n_m$. Thus, $s_{m,k}$ is bounded. According to $z_{m,k}=s_{m,k}+v_{m,k}$ and the boundedness of $v_{m,k}$, $z_{m,k}$ is bounded. Because of (16), $\hat{\Theta}_{m,k}$ is bounded. Due to $\Theta_{m,k}$ being constant, the estimation error $\tilde{\Theta}_{m,k}$ is also bounded. Thus, the boundedness of $\alpha_{m,k}$ and u_m are bounded, and $\zeta_{m,k}$ is also bounded. According to (9), $x_{m,k}$ and ∂_m are bounded. Since $G_{m,k}$ is a non-negative function, $\bar{\delta}_m\left(1-16\tanh^2\left(\frac{s_{m,k}}{\sigma_{m,k}}\right)\right)G_{m,k}$ is bounded and suppose G_{m0} is its upper bound. On the basis of (56), one obtains

$$\dot{V}\le -AV+\hat{\chi}_{n_m}, \tag{58}$$

where $\hat{\chi}_{n_m}=\chi_{n_m}+G_{m0}$. Furthermore, it can be obtained that $0\le V\le[V(0)-(\hat{\chi}_{n_m}/A)]e^{-At}+(\hat{\chi}_{n_m}/A)$. Consequently, all signals of the CLS are regulated to a compact set Ξ_1.

$$\Xi_1=\left\{(x_{m,k},z_{m,k},s_{m,k},\tilde{\Theta}_{m,k})\,||\,V\le\frac{\hat{\chi}_{n_m}}{A}\right\}.$$

Case B $s_{m,k}\notin\Omega_{m_k}$ for $1\le m\le M$ and $1\le k\le n_m$. In light of Lemma 4, one has $\bar{\delta}_m(1-16\tanh^2(s_{m,k}/m_k))G_{m,k}\le 0$. Thus, (56) yields

$$\dot{V}\le -AV+\chi_{n_m}. \tag{59}$$

The same as **Case A**, all signals of the CLS are regulated to a compact set Ξ_2.

$$\Xi_2=\left\{(x_{m,k},z_{m,k},s_{m,k},\tilde{\Theta}_{m,k})\,||\,V\le\frac{\chi_{n_m}}{A}\right\}.$$

To sum up the above, it can be concluded that all signals in the CLS remain SGUUB. According to the above discussions, the parameters selection guideline of the proposed control solution is given in Algorithm 1.

Remark 2 In contrast to the classical ETC utilized in References [10, 11, 26], which requires continuous monitoring of the measurement error to determine whether it needs to be triggered, the developed self-triggered control scheme avoids the use of an additional observer by obtaining the next trigger moment from the current one. In addition, although the self-triggered control approach can reduce the transmission cost, the stabilization performance of the control system may be weakened based on the control signal being discontinuous between two consecutive trigger moments. In particular, the interconnected nonlinear time-delay system has a relatively complicated structure. To this end, the FTPF is introduced to achieve the stabilization control goal, which also increases the challenges and difficulties of control design to a certain extent.

Remark 3 In this brief, the trial-and-error-based tactic for choosing the design parameters is utilized to achieve satisfactory control performance. By increasing the design parameters $c_{m,i}$, $\mu_{m,k}$, $\bar{r}_{m,1}$, and $\kappa_{m,k}$ or decreasing the design parameters Λ_m, E_m, and $\rho_{m,i}$ such that the stabilization error is as small as possible. Theoretically speaking, provided that the design parameters are larger, it may result in a larger amplitude of the control input. Therefore, it is essential to make a trade-off between control performance and control energy by choosing the design parameters appropriately.

Remark 4 Following the above discussion, we can derive that the control input $\bar{u}_m$ is bounded. Hence, $(\Lambda_m\,|\,\bar{u}_m(t)\,|+E_m)/(\max\{L_m,|\,\dot{v}_m(t)\,|\})$ is also bounded. Given the circumstances of (45), it is available that the lower bound for inter-execution intervals satisfies $t^*=t_{k+1}-t_k>0$, that is, excluding the Zeno-behavior.

Algorithm 1 The Parameters Selection Guideline

Step i: Select the number of neurons $K \geq 1$ and define the Gaussian function of RBFNN.

Step ii: The FTPF $\ell_m(t)$ design parameters $\ell_{m0} > 0, \ell_{mT_f} > 0$ and $T_f > 0$ are selected such that $\ell_m(0) = \ell_{m0} + \ell_{mT_f}$. The smaller the value of the parameter $\ell_{mT_f} > 0$ is selected, the smaller the stabilization error boundary in the steady response will be obtained.

Step iii: Specify the FOF to avoid the explosive calculation, and choose the parameters $k_{m,l1} > 0, k_{m,l2} > 0, k_{m,l3} > 0$ and $0 < P_m < 1$ to obtain a decent filter performance.

Step iv: Specify the error compensation signal, and select the design parameter $c_{m,i} > 0$ with $i = 1 \ldots, n_m$ to eliminate the filter errors.

Step v: Choose appropriate design parameters $c_{m,i} > 0, a_{m,i} > 0$ to determine the virtual control function $\alpha_{m,i}$ and the parameters $\mu_{m,i} > 0, \rho_{m,i} > 0$ to determine the adaptive laws $\dot{\hat{\Theta}}_{m,i}, 1 \leq i \leq n_m - 1$.

Step vi: Choose appropriate design parameters $c_{m,n_m} > 0, a_{m,n_m} > 0, 0 < \bar{\kappa}_m < 1, \underline{\zeta}_{m0} > 0$, and $u_m^{min} > 0$ to determine the virtual control function α_{m,n_m} and the parameters $\mu_{m,n_m} > 0, \rho_{m,n_m} > 0$ to determine the adaptive laws $\dot{\hat{\Theta}}_{m,n_m}$.

Step vii: Select appropriate design parameters $0 < \Lambda_m < 1, E_m > 0, \jmath_m > 0, \bar{E}_m > 0$, and $L_m > 0$ in the self-triggered mechanism such that $\bar{E}_m > E_m/(1 - \Lambda_m)$ to economize the communication resources.

Step viii: Select appropriate design parameter $u_m^{Max} > 0$ to constrain quantization input in the saturation function.

Step ix: Select appropriate design parameters $u_m^{min} > 0$ and $0 < \delta_m < 1$ in the hysteresis quantizer to reduce the effect of bandwidth limitation and chattering phenomenon.

4 Simulation example

In this section, two simulation examples are used to validate the effectiveness of the proposed adaptive self-triggered quantized control scheme.

Example 1 In the background of the chemical industry, two-stage chemical reactors are universally prevalent. However, it is well known that interconnected nonlinear systems consisting of two two-stage chemical reactors have significant application potential, which not only models more complex chemical reaction systems but also improves the overall conversion rate. To sum up, the nonlinear systems composed of two two-stage chemical systems have certain practical implications to some extent.

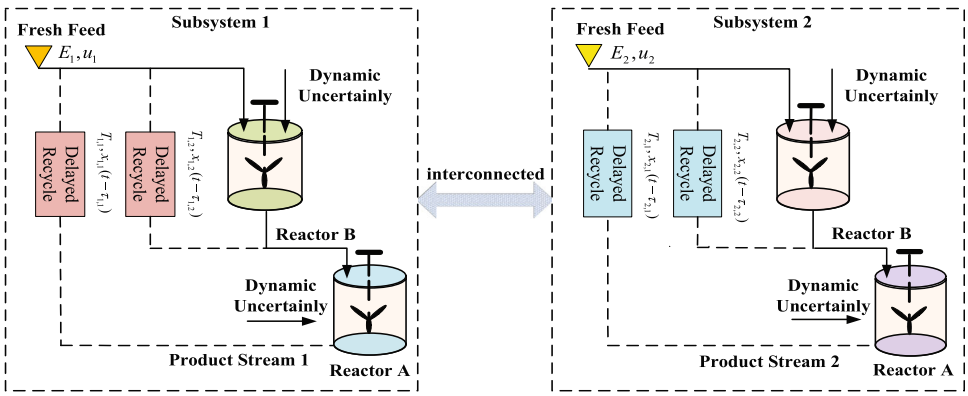

Fig. 1 Structure chart of a two-stage chemical reactors

Let us consider two-stage chemical reactors with dynamic uncertainly and delayed recycle streams, as exhibited in Fig. 1. As in [42], the mathematical model of the reactors can be expressed as:

$$\begin{cases} \dot{\psi}_1 = -\psi_1 + 0.5x_{1,1}^2 + 0.5, \\ \dot{x}_{1,1} = -\dfrac{1}{Y_{1,1}}x_{1,1} - \dfrac{1}{Y_{1,1}}x_{1,1}(t-\tau_{1,1}) + \dfrac{1-T_{1,2}}{M_{1,1}}x_{1,2} \\ \quad - H_{1,1}x_{1,1} + 0.1\sin(x_{1,1}+x_{2,1}) + \psi_1 x_{1,1}\sin(x_{1,1}), \\ \dot{x}_{1,2} = -\dfrac{1}{Y_{1,2}}x_{1,2}^2 + \dfrac{T_{1,1}}{M_{1,2}}x_{1,1}(t-\tau_{1,1}) - \dfrac{2Q_{1,2}^*}{Y_{1,2}}x_{1,2} \\ \quad + \dfrac{E_1}{M_{1,2}}q(u_1) - H_{1,2}x_{1,2} + \dfrac{T_{1,2}}{M_{1,2}}x_{1,2}(t-\tau_{1,2}) \\ \quad + 0.2\sin(x_{2,1}) + \psi_1 x_{1,1}x_{1,2}, \\ \dot{\psi}_2 = -\psi_2 + 0.5x_{2,1}^2 + 0.5, \\ \dot{x}_{2,1} = -\dfrac{1}{Y_{2,1}}x_{2,1} - \dfrac{1}{Y_{2,1}}x_{2,1}(t-\tau_{2,1}) + \dfrac{1-T_{2,2}}{M_{2,1}}x_{2,2} \\ \quad - H_{2,1}x_{2,1} + 0.1\sin(x_{1,1}) + \psi_2 x_{2,1}\sin(x_{2,1}), \\ \dot{x}_{2,2} = -\dfrac{1}{Y_{2,2}}x_{2,2}^2 + \dfrac{T_{2,1}}{M_{2,2}}x_{2,1}(t-\tau_{2,1}) - \dfrac{2Q_{2,2}^*}{Y_{2,2}}x_{2,2} \\ \quad + \dfrac{E_2}{M_{2,2}}q(u_2) - H_{2,2}x_{2,2} + \dfrac{T_{2,2}}{M_{2,2}}x_{2,2}(t-\tau_{2,2}) \\ \quad + 0.2\sin(x_{1,1}-x_{2,1}) + \psi_2 x_{2,1}\sin(x_{2,2}), \end{cases}$$

where $x_{m,1}$ and $x_{m,2}$ $(m = 1, 2)$ are the compositions to be controlled; $q(u_m)$ is the quantized signal; the representation and values of the system parameters are shown in Table 1.

To confirm the validity of Assumption 2 for ψ_m-dynamic, let us choose $\check{V}_m(\psi_m) = \psi_m^2$, then

$$\begin{aligned} \dot{\check{V}}_m(\psi_m) &= 2\psi_m(-\psi_m + 0.5x_{m,1}^2 + 0.5) \\ &\le -2\psi_m^2 + \frac{1}{4l_m}\psi_m^2 + \frac{1}{l_m}\psi_m^2 + l_m x_{m,1}^4 + \frac{1}{4}l_m. \end{aligned}$$

By selecting $l_m = 2.5$, results in

$$\dot{\check{V}}_m(\psi_m) \le -1.5\psi_m^2 + 2.5x_{m,1}^4 + 0.625.$$

Define $\Upsilon_{m,1}(|\psi_m|) = 0.6\psi_m^2$, $\Upsilon_{m,2}(|\psi_m|) = 0.5\psi_m^2$, $r_{m,1} = 1.5$, $r_{m,2} = 0.625$, and $\pi_{m0}(\|x_{m,1}\|) = 2.5x_{m,1}^4$, Assumption 2 is certified successful. On the basis of Lemma 1 and taking $\bar{r}_{m,1} = 1.2 \in (0, r_{m,1})$, a dynamic signal λ_m is represented as:

$$\dot{\lambda}_m = -1.2\lambda_m + 2.5x_{m,1}^4 + 0.625.$$

Following the control design in Sect. 3, the corresponding design parameters are identified in Table 2. To intuitively show the superiority of the proposed methodology, a comparison simulation between the proposed approach and the algorithm in [16] is exhibited in Figs. 2, 3, 4, 5, and 6. Specifically, the states $x_{m,1}$ and $x_{m,2}$ $(m = 1, 2)$ are shown for each subsystem in Fig. 2. Figure 3 plots the profiles of system output $x_{m,1}$ for each subsystem. From Figs. 2 and 3, it is evidence obtained that the system states are SGUUB and system output $x_{m,1}$ can converge better to a predetermined range $(-\ell_m, \ell_m)$ than the method in [16] in finite time. Furthermore, the response curves of the adaptive parameters $\hat{\Theta}_{m,1}$ and $\hat{\Theta}_{m,2}$ are depicted for each subsystem in Fig. 4. Figure 5 illustrates the graphs of the

Table 1 The model parameters

Notation	Representation	Value	Unit
$T_{m,1}/T_{m,2}$	The recycle flow rates	0.5	m^3/s
$H_{m,1}/H_{m,2}$	The reaction constants	0.5	$1/s$
$M_{m,1}/M_{m,2}$	The reactor volumes	0.5	m^3
$Q_{m,2}^*$	The equilibrium point	7/3	m^3
E_m	The feed rate	0.5	m^3/s
$Y_{m,1}/Y_{m,2}$	The reactor residence times	2	s

Table 2 The design parameters

The initial conditions
$x_{1,1}(0) = x_{2,1}(0) = 0.35, x_{1,2}(0) = x_{2,2}(0) = 1, \psi_1(0) = \psi_2(0) = 0,$ $\hat{\Theta}_{m,1}(0) = \hat{\Theta}_{m,2}(0) = 0, v_{m,1}(0) = v_{m,2}(0) = 0, \lambda_1(0) = \lambda_2(0) = 0.1$
The controller parameters
$c_{1,1} = 5, c_{1,2} = 4, c_{2,1} = c_{2,2} = 7, a_{m,1}^2 = a_{m,2}^2 = 0.5,$ $\Lambda_m = 0.1, L_m = 0.12,$ $\rho_{m,1} = \rho_{m,2} = 2, u_m^{\min} = 0.5, \delta_m = 0.2, \jmath_m = 1, E_m = 0.1, P_m = 0.9,$ $\ell_{m0} = 1, T_f = 1, \ell_{mT_f} = 0.1, \mu_{m,1} = \mu_{m,2} = 1, \bar{E}_m = 1,$
The time delays
$\tau_{m,1} = 0.2 + 0.08\sin(2t), \tau_{m,2} = 0.3 + 0.12\sin(2t).$
The Gaussian functions
$\psi_{m,i}^{\iota}(\bar{z}_{m,i}) = \exp\left[-((\bar{z}_{m,i}+\iota)^2/1)\right], i = 1, 2; \iota = 0, \pm1, \pm2, \pm3, \pm4,$ $\bar{z}_{m,1} = [x_{m,1}, s_{m,1}, p_m, \lambda_1(t)]^{\mathrm{T}}, \bar{z}_{m,2} = [x_{m,2}, s_{m,2}, \lambda_2(t), \dot{\zeta}_{m,2}]^{\mathrm{T}}.$

control input v_m and quantized input $q(u_m)$ for each subsystem. It can be seen that the quantization amplitude of the proposed control method is relatively small. Figure 6 expresses the trigger interval for each subsystem. To sum up, the proposed FTPP quantized control approach is superior to that investigated in [16] for achieving a better trade-off between the networked control and stability performance, and also excluding the Zeno phenomenon.

Example 2 Consider the following interconnected nonlinear time-delay plants:

$$\begin{cases}
\dot{\psi}_1 = -\psi_1 + 0.5x_{1,1}^2 + 0.5, \\
\dot{x}_{1,1} = x_{1,2} + \dfrac{x_{1,1} - x_{1,1}^3}{1 + x_{1,1}^2} + 0.1\sin(x_{1,1} + x_{2,1}) \\
\qquad - 0.5x_{1,1}(t - \tau_{1,1}) + \psi_1 x_{1,1}\sin(x_{1,1}), \\
\dot{x}_{1,2} = q(u_1) - (x_{1,1}^2 + 2x_{1,2})\sin(x_{1,1}) + x_{1,2}(t - \tau_{1,2}) \\
\qquad + 0.2\sin(x_{2,1}) + \psi_1 x_{1,1}x_{1,2}, \\
\dot{\psi}_2 = -\psi_2 + 0.5x_{2,1}^2 + 0.5, \\
\dot{x}_{2,1} = x_{2,2} + \dfrac{x_{2,1} - x_{2,1}^3}{1 + x_{2,1}^2} - 0.5x_{2,1}(t - \tau_{2,1}) + 0.1\sin(x_{1,1}) \\
\qquad + \psi_2 x_{2,1}\sin(x_{2,1}), \\
\dot{x}_{2,2} = q(u_2) - (x_{2,1}^2 + 2x_{2,2})\sin(x_{2,1}) + x_{2,2}(t - \tau_{2,2}) \\
\qquad + 0.2\sin(x_{1,1} - x_{2,1}) + \psi_2 x_{2,1}\sin(x_{2,2}), \\
\dot{\psi}_3 = -\psi_3 + 0.5x_{3,1}^2 + 0.5, \\
\dot{x}_{3,1} = x_{3,2} + \dfrac{x_{3,1} - x_{3,1}^3}{1 + x_{3,1}^2} - 0.5x_{3,1}(t - \tau_{3,1}) \\
\qquad + 0.1\sin(x_{1,1} + x_{3,1}) + \psi_3 x_{3,1}\sin(x_{3,1}), \\
\dot{x}_{3,2} = q(u_3) - (x_{3,1}^2 + 2x_{3,2})\sin(x_{3,1}) + x_{3,2}(t - \tau_{3,2}) \\
\qquad + 0.2\sin(x_{2,1} - x_{3,1}) + \psi_3 x_{3,1}\sin(x_{3,2}),
\end{cases}$$

where $f_{m,1} = (x_{m,1} - x_{m,1}^3)/(1 + x_{m,1}^2)$, $f_{m,2} = -(x_{m,1}^2 + 2x_{m,2})\sin(x_{m,1})$. $g_{1,1} = 0.1\sin(x_{1,1} + x_{2,1})$, $g_{1,2} = 0.2\sin(x_{2,1})$, $g_{2,1} = 0.1\sin(x_{1,1})$, $g_{2,2} = 0.2\sin(x_{1,1} - x_{2,1})$, $g_{3,1} = 0.1\sin(x_{1,1} + x_{3,1})$, $g_{3,2} = 0.2\sin(x_{2,1} - x_{3,1})$. $\Delta_{1,1} = \psi_1 x_{1,1}\sin(x_{1,1})$, $\Delta_{1,2} = \psi_1 x_{1,1}x_{1,2}$, $\Delta_{2,1} = \psi_2 x_{2,1}\sin(x_{2,1})$, $\Delta_{2,2} = \psi_2 x_{2,1}\sin(x_{2,2})$, $\Delta_{3,1} = \psi_3 x_{3,1}\sin(x_{3,1})$, $\Delta_{3,2} = \psi_3 x_{3,1}\sin(x_{3,2})$.
$\tau_{m,1} = 0.2 + 0.08\sin(2t)$, $\tau_{m,2} = 0.3 + 0.12\sin(2t)$.

We select the ψ_m-dynamic, the RBFNN basis function, virtual control signals, and adaptive laws of the numerical simulations like Example 1. The different parameters related to Example 1 are selected as follows:$x_{m,1}(0) = 0.2$, $x_{m,2}(0) = 1.2$, $c_{m,1} = c_{m,2} = 5$ $(m = 1, 2, 3)$. To further illustrate the stabilization performance investigated in this paper, the responses of the states $x_{m,1}$ and $x_{m,2}$ $(m = 1, 2, 3)$ are exhibited for each subsystem in Fig. 7. Figure 8 depicts the graphs of system output $x_{m,1}$ for each subsystem. The investigated self-triggered control scheme can guarantee that the system states in the resulting CLS are SGUUB and system output $x_{m,1}$ can regulated to a predetermined range $(-\ell_m, \ell_m)$ in finite time. In addition, the response curves of the adaptive parameters $\hat{\Theta}_{m,1}$ and $\hat{\Theta}_{m,2}$

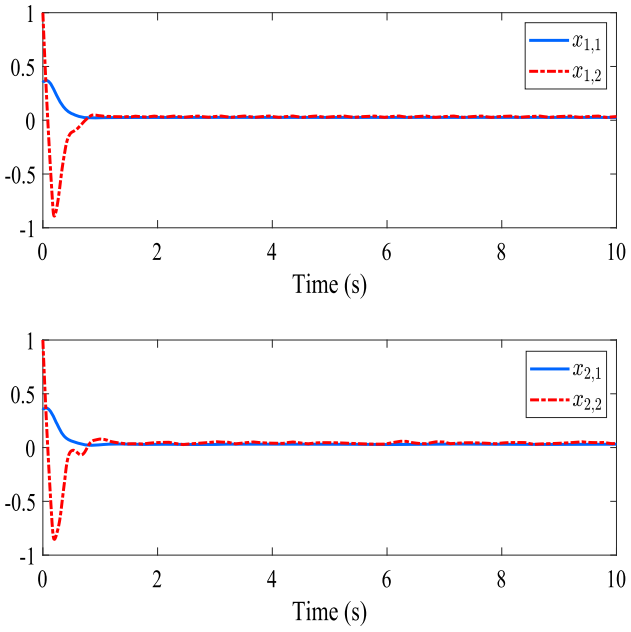

Fig. 2 System states $x_{m,1}$ and $x_{m,2}$

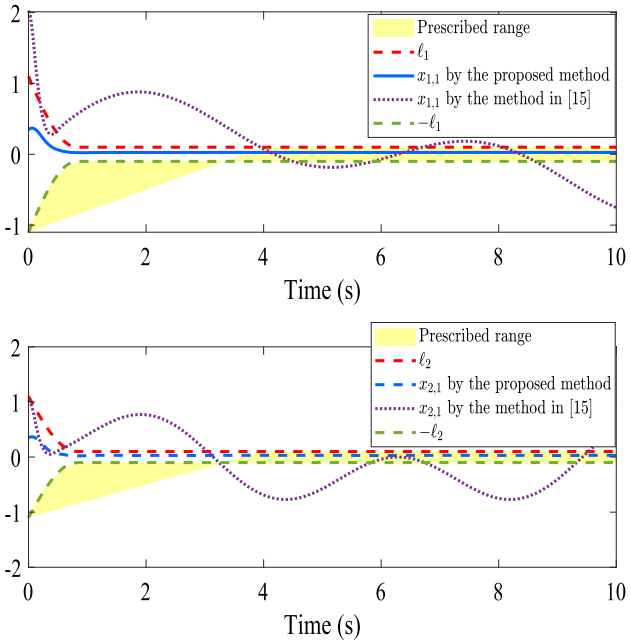

Fig. 3 System output $x_{m,1}$

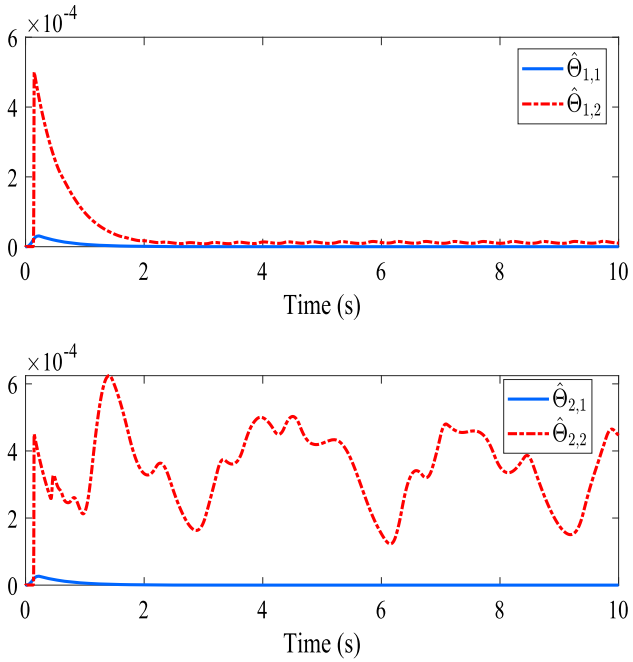

Fig. 4 Adaptive parameters $\hat{\Theta}_{m,1}$ and $\hat{\Theta}_{m,2}$

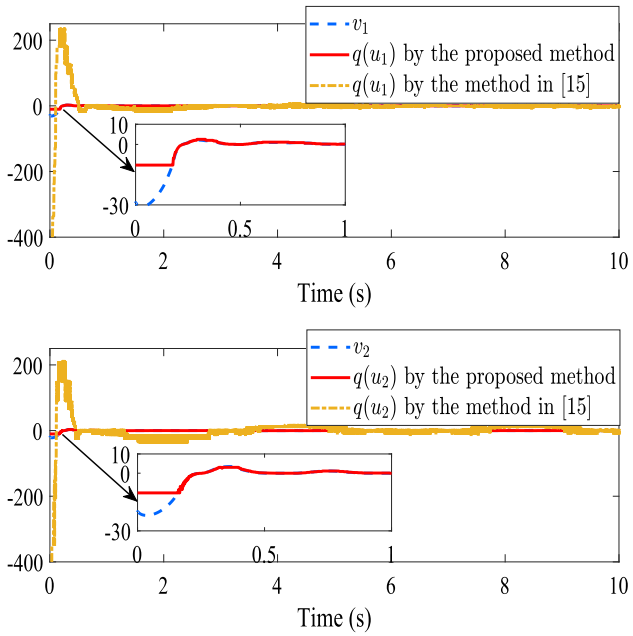

Fig. 5 Control signal v_m and quantized signal $q(u_m)$

are shown for each subsystem in Fig. 9. Figure 10 plots the graphs of the control input v_m and quantized input $q(u_m)$ for each subsystem. Figure 11 exhibits the trigger interval for each subsystem. To sum up, the presented self-triggered control approach can achieve a better trade-off between

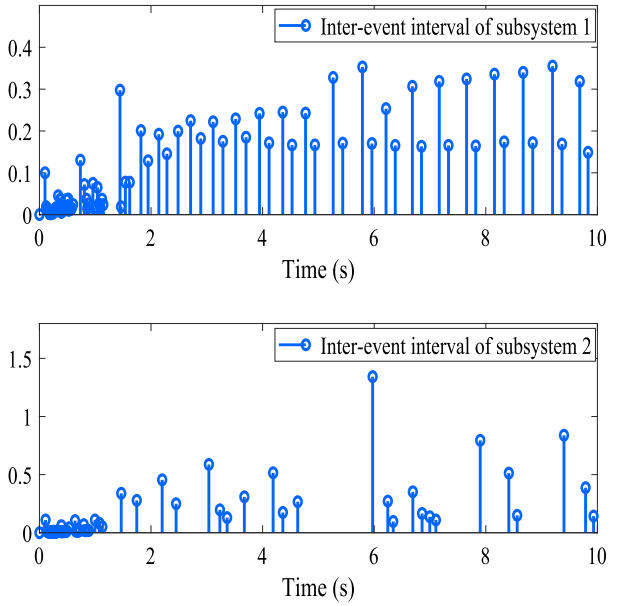

Fig. 6 Inter-event intervals

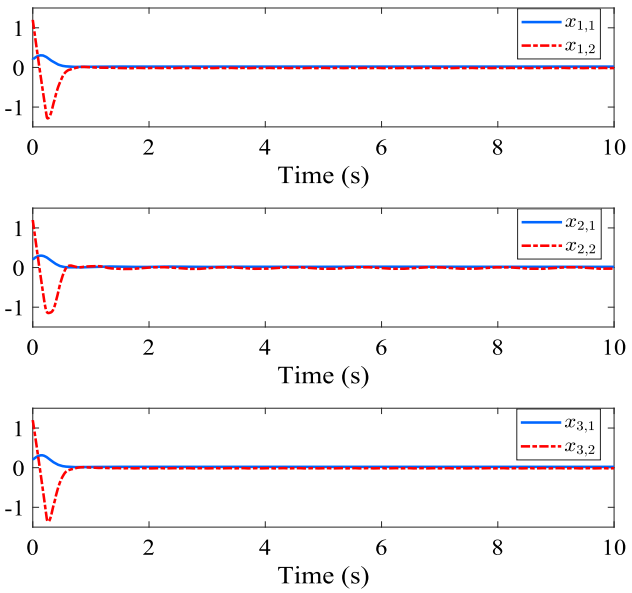

Fig. 7 System states $x_{m,1}$ and $x_{m,2}$

networked control and stability performance, and the Zeno phenomenon is also ruled out.

5 Conclusion

Self-triggered-based adaptive neural decentralized control strategy for interconnected nonlinear time-delay systems involving finite-time prescribed performance has been

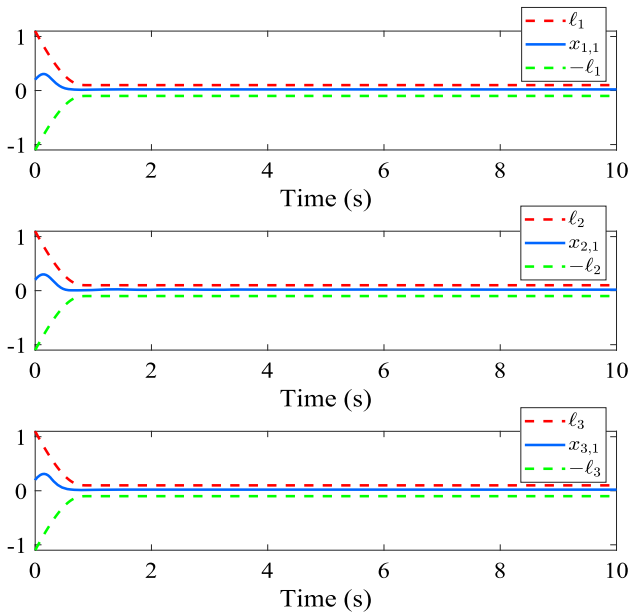

Fig. 8 System output $x_{m,1}$

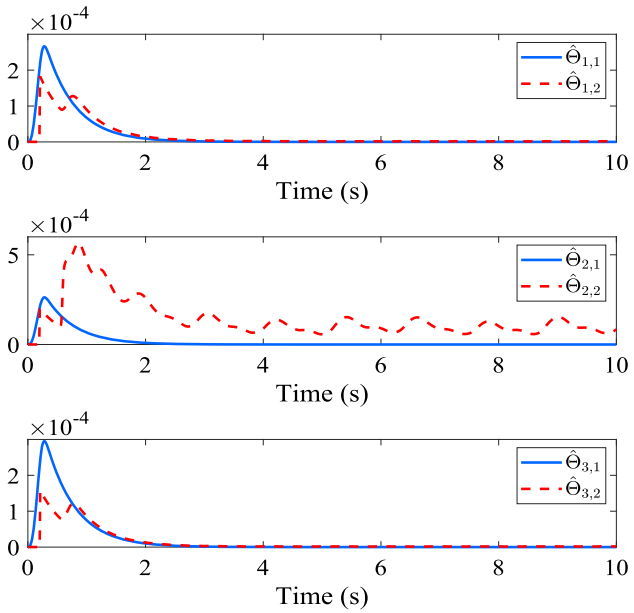

Fig. 9 Adaptive parameters $\hat{\Theta}_{m,1}$ and $\hat{\Theta}_{m,2}$

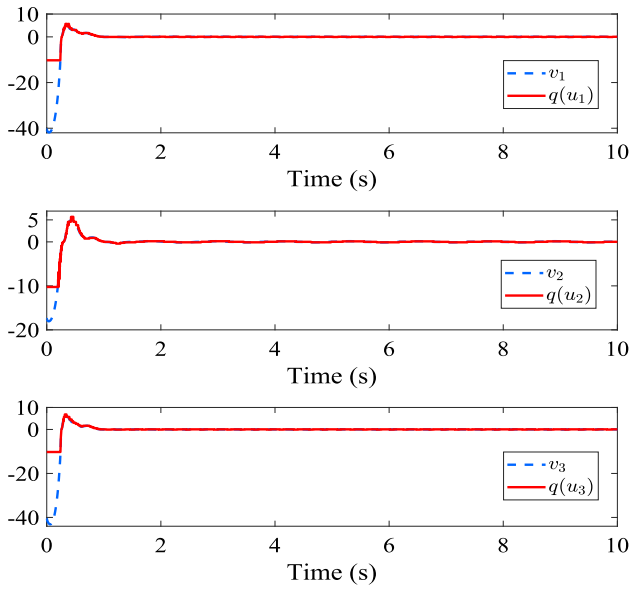

Fig. 10 Control signal v_m and quantized signal $q(u_m)$

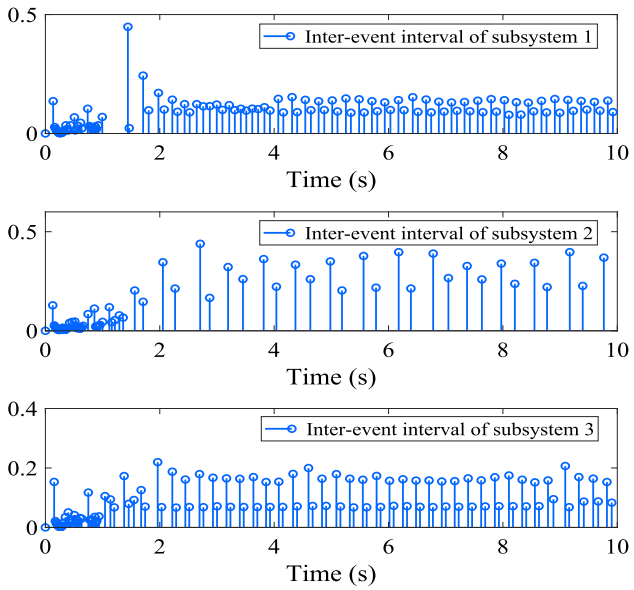

Fig. 11 Inter-event intervals

developed. By utilizing the hyperbolic tangent function and RBFNNs, the potential singularity issue has been eliminated. Meanwhile, an improved FOF was incorporated into the controller design, which can avoid the tremendous " amount of calculation " and the adverse impact of filter error has been excluded. Besides, the effect of bandwidth limitation was considered in the self-triggered adaptive FTPP control scheme, achieving a trade-off between stability performance and networked control. The presented controller ensured all signals in CLS are SGUUB, and the system output fluctuated to a small adjustable range within a finite time interval. Last but not least, the effectiveness and superiority of the proposed scheme have been verified by two simulation examples. In the future, the author will work to consider the self-triggered adaptive secure control issue for interconnected nonlinear time-delay systems with cyberattacks. In addition, inspired by [43] in dealing with the tracking of small-amplitude signals, a straightforward and effective nonlinearity is implemented in the controller, resulting in better signal-to-noise ratio performance, which will be another topic for our future research.

Acknowledgements This work was supported in part by the National Natural Science Foundation of China under Grants 61976081 and 62203153, in part by the Natural Science Fund for Excellent Young Scholars of Henan Province under Grant 202300410127, in part by Key Scientific Research Projects of Higher Education Institutions in Henan Province under Grant 22A413001, in part by Top Young Talents in Central Plains under Grant Yuzutong (2021) 44, in part by Technology Innovative Teams in University of Henan Province under Grant 23IRTSTHN012, in part by the Natural Science Fund for Young Scholars of Henan Province under Grant 222300420151, and in part by the Serbian Ministry of Education, Science and Technological Development (No. 451-03-68/2022-14/200108).

Data availability statements Data sharing is not applicable to this article as no datasets were generated or analysed during the current study.

Declarations

Conflict of interest The authors declared that they have no conflicts of interest in this work. We declare that we do not have any commercial or associative interest that represents a conflict of interest in connection with the work submitted.

References

1. Tong S, Li Y, Liu Y (2021) Observer-based adaptive neural networks control for large-scale interconnected systems with nonconstant control gains. IEEE Trans Neural Netw Learn Syst 32(4):1575–1585
2. Hamdy M, ElGhazaly G (2014) Adaptive neural decentralized control for strict feedback nonlinear interconnected systems via backstepping. Neural Comput Appl 24:259–269
3. Zhu S, Han Y (2022) Adaptive decentralized prescribed performance control for a class of large-scale nonlinear systems subject to nonsymmetric input saturations. Neural Comput Appl 34:11123–11140
4. Li X, Yang G (2017) Adaptive decentralized control for a class of interconnected nonlinear systems via backstepping approach and graph theory. Automatica 76:87–95
5. Swaroop D, Hedrick JK, Yip PP, Gerdes JC (2000) Dynamic surface control for a class of nonlinear systems. IEEE Trans Autom Control 45(10):1893–1899
6. Tabatabaei SM, Kamali S, Arefi MM, Cao J (2020) Prescribed performance adaptive DSC for a class of time-delayed switched nonlinear systems in nonstrict-feedback form: Application to a two-stage chemical reactor. J Process Control 89:85–94
7. Cheng T, Niu B, Zhang J, Wang D, Wang Z (2021) Time-/event-triggered adaptive neural asymptotic tracking control of nonlinear interconnected systems with unmodeled dynamics and prescribed performance. IEEE Trans Neural Netw Learn Syst. https://doi.org/10.1109/TNNLS.2021.3129228
8. Farrell JA, Polycarpou M, Sharma M, Dong W (2009) Command filtered backstepping. IEEE Trans Autom Control 54(6):1391–1395
9. Lu S, Chen M, Liu Y, Shao S (2022) Adaptive NN tracking control for uncertain MIMO nonlinear system with time-varying state constraints and disturbances. IEEE Trans Neural Netw Learn Syst. https://doi.org/10.1109/TNNLS.2022.3141052
10. Song S, Park JH, Zhang B, Song X (2022) Event-based adaptive fuzzy fixed-time secure control for nonlinear CPSs against unknown false data injection and backlash-like hysteresis. IEEE Trans Fuzzy Syst 30(6):1939–1951
11. Liu L, Liu YJ, Tong S, Gao Z (2022) Relative threshold-based event-triggered control for nonlinear constrained systems with application to aircraft wing rock motion. IEEE Trans Ind Inf 18(2):911–921
12. Li X, Wu H, Cao J (2023) Prescribed-time synchronization in networks of piecewise smooth systems via a nonlinear dynamic event-triggered control strategy. Math Comput Simul 203:647–668
13. Wang J, Zhang H, Ma K, Liu Z, Chen CP (2022) Neural adaptive self-triggered control for uncertain nonlinear systems with input hysteresis. IEEE Trans Neural Netw Learn Syst 33(11):6206–6214
14. Chen W, Wang J, Ma K, Wu W (2022) Adaptive self-triggered control for a nonlinear uncertain system based on neural observer. Int J Control 95(7):1922–1932
15. Hayakawa T, Ishii H, Tsumura K (2009) Adaptive quantized control for linear uncertain discrete-time systems. Automatica 45(3):692–700
16. Sun H, Hou L, Zong G, Yu X (2020) Adaptive decentralized neural network tracking control for uncertain interconnected nonlinear systems with input quantization and time delay. IEEE Trans Neural Netw Learn Syst 31(4):1401–1409
17. Liu W, Lim C, Shi P, Xu S (2017) Backstepping fuzzy adaptive control for a class of quantized nonlinear systems. IEEE Trans Fuzzy Syst 25(5):1090–1101
18. Sun W, Su S, Xia J, Zhuang G (2021) Command filter-based adaptive prescribed performance tracking control for stochastic uncertain nonlinear systems. IEEE Trans Syst Man Cybern Syst 51(10):6555–6563
19. Song X, Sun P, Song S, Stojanovic V (2022) Event-driven NN adaptive fixed-time control for nonlinear systems with guaranteed performance. J Franklin Inst 359(9):4138–4159
20. Tong D, Liu X, Chen Q, Zhou W, Liao K (2022) Observer-based adaptive finite-time prescribed performance NN control for nonstrict-feedback nonlinear systems. Neural Comput Appl 34:12789–12805
21. Wang H, Bai W, Zhao X, Liu PX (2022) Finite-time-prescribed performance-based adaptive fuzzy control for strict-feedback nonlinear systems with dynamic uncertainty and actuator faults. IEEE Trans Cybern 52(7):6959–6971
22. Yan H, Li Y (2017) Adaptive NN prescribed performance control for nonlinear systems with output dead zone. Neural Comput Appl 28:145–153
23. Wang T, Tong S, Li Y (2013) Adaptive neural network output feedback control of stochastic nonlinear systems with dynamical uncertainties. Neural Comput Appl 23:1481–1494
24. Zhang L, Zhu L, Hua C, Qian C (2022) Adaptive decentralized control for interconnected time-delay uncertain nonlinear systems with different unknown control directions and deferred full-state constraints. IEEE Trans Neural Netw Learn Syst. https://doi.org/10.1109/TNNLS.2022.3171518
25. Mao J, Huang S, Xiang Z (2017) Adaptive tracking control for a class of non-affine switched stochastic nonlinear systems with unmodeled dynamics. Neural Comput Appl 28:1069–1081
26. Li M, Li S, Ahn CK, Xiang Z (2022) Adaptive fuzzy event-triggered command-filtered control for nonlinear time-delay systems. IEEE Trans Fuzzy Syst 30(4):1025–1035
27. Yu J, Shi P, Zhao L (2018) Finite-time command filtered backstepping control for a class of nonlinear systems. Automatica 92:173–180
28. Liu Y, Liu X, Jing Y (2018) Adaptive neural networks finite-time tracking control for non-strict feedback systems via prescribed performance. Inf Sci 468:29–46
29. Podlubny I (1998) Fractional differential equations. Academic, New York

30. Zhou J, Wen C, Yang G (2014) Adaptive backstepping stabilization of nonlinear uncertain systems with quantized input signal. IEEE Trans Autom Control 59(2):460–464
31. Jiang ZP, Praly L (1998) Design of robust adaptive controllers for nonlinear systems with dynamic uncertainties. Automatica 34(7):825–840
32. Tong S, Li Y (2010) Robust adaptive fuzzy backstepping output feedback tracking control for nonlinear system with dynamic uncertainties. Sci China Inf Sci 53:307–324
33. Polycarpou MM (1996) Stable adaptive neural control scheme for nonlinear systems. IEEE Trans Autom Control 41(3):447–451
34. Wang M, Chen B, Shi P (2008) Adaptive neural control for a class of perturbed strict-feedback nonlinear time-delay systems. IEEE Trans Syst Man Cybern Part B 38(3):721–730
35. Wang LX (1993) Stable adaptive fuzzy control of nonlinear systems. IEEE Trans Fuzzy Syst 1(2):146–155
36. Song X, Sun P, Song S, Wu Q, Lu J (2023) Event-triggered fuzzy adaptive fixedtime output-feedback control for nonlinear systems with multiple objective constraints. Int J Fuzzy Syst. 25:275-288
37. Liu H, Pan Y, Cao J, Wang H, Zhou Y (2020) Adaptive neural network backstepping control of fractional-order nonlinear systems with actuator faults. IEEE Trans Neural Netw Learn Syst 31(12):5166–5177
38. Li Y, Chen Y, Podlubny I (2009) Mittag–Leffler stability of fractional order nonlinear dynamic systems. Automatica 45(8):1965–1969
39. Song S, Park JH, Zhang B, Song X (2022) Composite adaptive fuzzy finite-time quantized control for full state-constrained nonlinear systems and its application. IEEE Trans Syst Man Cybernet Syst 52(4):2479–2490
40. Zhou Q, Shi P, Tian Y, Wang M (2015) Approximation-based adaptive tracking control for MIMO nonlinear systems with input saturation. IEEE Trans Cybern 45(10):2119–2128
41. Knuth DE (1997) The art of computer programming. Addison-Wesley, Reading
42. Hua C, Liu PX, Guan X (2009) Backstepping control for nonlinear systems with time delays and applications to chemical reactor systems. IEEE Trans Ind Electron 56(9):3723–3732
43. Bucolo M, Buscarino A, Fortuna L, Gagliano S (2021) Can noise in the feedback improve the performance of a control system? J Phys Soc Jpn 90(7):075002